Platelet microparticles mediate the glomerular endothelial injury in early diabetic nephropathy

Yang Zhang[1], Kun Ling Ma[1, *], Yu Xiang Gong[1], Gui Hua Wang[1], Ze Bo Hu[1], Liang Liu[1], Jian Lu[1], Pei Pei Chen[1], Chen Chen Lu [1], Xiong Zhong Ruan[2], Bi Cheng Liu[1]

[1]Institute of Nephrology, Zhongda Hospital, School of Medicine, Southeast University, Nanjing, 210009, China;

[2]Centre for Nephrology, University College London (UCL) Medical School, Royal Free Campus, UK.

* Correspondence: Dr. Kun Ling Ma, Institute of Nephrology, Zhongda Hospital, School of Medicine, Southeast University, Nanjing, 210009, China. Email: klma05@163.com

Keywords Platelet microparticles, diabetic nephropathy, glomerular endothelial injury, mTORC1 pathway, CXCL7

Running title Platelet microparticles and diabetic nephropathy

Abstract **Background** Glomerular endothelium dysfunction plays crucial roles in the pathogenesis of early diabetic nephropathy (DN) and might be caused by circulating metabolic abnormalities. Platelet microparticles (PMPs) are extracellular vesicles released from activated platelets and have recently emerged as a novel regulator of vascular dysfunction. This study aimed to investigate the effects of PMPs on glomerular endothelial injury in early DN. **Methods** Streptozotocin-induced diabetic rat model and primary rat glomerular endothelial cells (GEnCs) were used for experiments. Isolated PMPs were measured by flow cytometry. **Results** Plasma PMPs were significantly increased in diabetic rats, which was inhibited by aspirin. In cultured GEnCs, PMPs induced the production of reactive oxygen, decreased nitric oxide level, inhibited the activities of endothelial nitric oxide synthase and superoxide dismutase, decreased the barrier permeability of the GEnCs, and reduced the thickness of endothelial surface layer. Conversely, inhibition of PMPs *in vivo* by aspirin improved glomerular endothelial injury. Further analysis showed that PMPs activated the mammalian target of rapamycin complex 1 (mTORC1) pathway in GEnCs and inhibition of the mTORC1 pathway by rapamycin or raptor siRNA significantly protected against PMPs-induced glomerular endothelial injury *in vivo* and *in vitro*. Moreover, PMPs contributed to glomerular endothelial injury induced by PMP-derived chemokine (C-X-C motif) ligand 7 (CXCL7), and antagonizing CXCL7 using CXCL7 neutralizing antibody or blocking CXCL7 receptor by SB225002 dramatically attenuated PMPs-induced glomerular endothelial injury. **Conclusions** These findings demonstrate a pathogenic role of PMPs in glomerular endothelium dysfunction, which might be a potential therapeutic target for the treatment of early DN.

Introduction

Diabetic nephropathy (DN) is one of the most common microvascular complications of diabetes.[1] Despite increasing research progress in the treatment of DN, the incidence and prevalence of end-stage renal disease (ESRD) are rapidly rising worldwide.[2-4]

The glomerular endothelium is the first layer of the glomerular filtration barrier (GFB), consisting of glomerular endothelial cells (GEnCs), the endothelial surface layer (ESL) and fenestrations, and tight junctions among cells.[5] GEnCs are highly specialized cells characterized by the presence of 60-80 nm transcellular fenestrations and covered with ESL.[6, 7] Glycocalyx is the main component of the ESL, which covers both fenestral and inter-fenestral domains of the GEnC luminal surface.[5-7] The fenestrations and covered glycocalyx with characteristics of the molecular and charge barrier are essential for selective permeability.[7, 8] The glomerular endothelium is encountered by plasma and forms the first barrier to macromolecular substances. In addition, the glomerular endothelium makes an important contribution to maintaining the homeostasis within the glomerulus in response to haemodynamic changes by secreting vasoactive substances. It is increasingly recognized that glomerular endothelial dysfunction is an early and deleterious hallmark of DN, resulting in impairment of the GFB and the appearance of albuminuria.[7, 9, 10] The thickness of the glycocalyx and mean percentage of fenestrations in glomerular endothelium were reduced in DN, which was correlated tightly with the permeability of the GFB and albuminuria.[11, 12] Improvement of glomerular glycocalyx by inhibiting the heparanase level reduced glomerular

permselectivity and the development of albuminuria.[13] Recent studies have shown that endothelial nitric oxide synthase (eNOS) knockout mice develop aggravated DN with extensive mesangial expansion and severe podocyte injury, suggesting a causal link between endothelial dysfunction and the onset of early DN.[14, 15] However, the initiating factors and related mechanisms of glomerular endothelial injury in early DN are still unclear.

Platelet microparticles (PMPs) are extracellular vesicles (EVs) derived from activated platelets that range in size from 0.1 to 1 μm in diameter.[16-18] PMPs account for 70%–90% of all the circulating microparticles.[16] PMPs enriched in proteins, lipids, and genetic information derived from activated platelets have the ability to modify the phenotype and function of the target cells.[19-21] PMPs increase the expression of intercellular adhesion molecule-1 (ICAM-1) in endothelial cells by delivering arachidonic acid and inflammatory cytokines, leading to monocyte adherence to the vessel wall.[22] In the condition of diabetes, the levels of circulating MPs are highly elevated, strongly associated with the urinary albumin excretion rate.[23-26] However, whether PMPs contribute to glomerular endothelium dysfunction in early DN is still unknown.

Therefore, this study aimed to investigate the role of PMPs in glomerular endothelial injury at the early stage of DN and to explore its underlying mechanisms.

Concise Methods

Animals

Male Sprague-Dawley (SD) rats weighing 200-220 g were obtained from Shanghai Bikai Company (China). The rats were maintained under a constant 12-hour photoperiod at temperatures ranging from 21-23°C and allowed free access to food and water, acclimatized for at least a week before further operation. All protocols, including diabetes induction and sacrifice operation, were approved by the Institutional Animal Care and Use Committee of Southeast University.

Diabetes was induced by streptozotocin (STZ) injection as described previously.[27] Briefly, rats were injected with 60 mg/kg body weight of STZ (Sigma, USA) once intraperitoneally. After 72 hours of STZ injection, blood glucose levels were measured, and rats with a blood glucose level higher than 16.7 mmol/l were diagnosed as diabetic rats. For the normal controls, rats were injected with 0.1 mol/l sodium citrate buffer once intraperitoneally. At week 3 after diabetes induction, the rats were divided into four groups (n=10): normal controls treated with vehicle (Ctrl), diabetic rats treated with vehicle (DM), diabetic rats treated with aspirin (15 mg/kg) (DM+Asp), and diabetic rats treated with rapamycin (1 mg/kg) (DM+Rapa). Aspirin was given by intragastric administration daily in the whole study period. Body weight and 24-hour urine volume were determined weekly until being killed at the week 4, 8, and 12. The concentrations of blood urea nitrogen (BUN) and serum creatinine were determined using automatic analysers (Hitachi, Japan). Urinary albumin levels were measured using an enzyme-linked immunosorbent assay.

GEnC isolation, culture, and identification

Glomeruli were isolated from rat kidneys under sterile conditions by differential sieving as previously described.[28] Briefly, male SD rats (150-200 g) were anaesthetized by an intraperitoneal injection of chloral hydrate (400 mg/kg). Kidneys were isolated and placed into cold sterile Hank's solution. After tearing the renal capsule from the lavaged kidney, the renal cortex was cut into 1-2-mm^3-thick fragments. The kidney tissues were ground with a 100-mesh stainless steel sieve, followed by filtering through 150 and 200-mesh steel sieves, respectively. Glomeruli in the 200-mesh steel sieve were collected and centrifuged at 460 g for 5 minutes. After two washes with serum-free Dulbecco's Modified Eagle's Medium (DMEM), the glomeruli were treated with type IV collagenase (1 g/L) for 30 minutes at 37°C and then centrifuged at 460 g for 5 minutes. The supernatant was eliminated, and the pellet was washed twice with serum-free DMEM to collect the glomeruli. The glomeruli were seeded in a culture flask pre-coated with 10 μg/ml collagen Ⅰ and the prepared endothelial cell medium. The endothelial cell medium was replaced every 3 days, and the GEnCs were grown in a confluent monolayer during the second week. Identification of GEnCs was made using immunofluorescent staining (Supplemental Figure 3).

For the mTORC1 pathway inhibition, GEnCs were treated with 10 ng/ml Rapamycin (Sigma, USA) or transfected with raptor siRNA using Lipofectamine 2000 (Invitrogen, USA) per the recommendations of the manufacturer.

The isolation of circulating microparticles

Circulating microparticles (MPs) were separated according to the method reported by Dasgupta *et al*.[29] Briefly, circulating MPs were isolated by differential centrifugation. Blood was sampled by right heart puncture using 10 ml syringe and then added to polypropylene tubes with 0.129 mol/l sodium citrate. Platelet-rich plasma (PRP) was obtained by centrifugation at 1000 g for 15 minutes at 18°C. The PRP was then centrifuged at 5000 g for 15 minutes at 18°C to obtain platelet-free plasma (PFP). The PFP was further centrifuged using an Eppendorf 5424R centrifuge machine at 20000 g for 30 minutes to precipitate MPs at 18°C. The pellets containing MPs were suspended in modified Tyrode's buffer(MTB) and stored at -80°C.

Measurement of circulating PMPs

To label PMPs, resuspension solution containing MPs was incubated with allophycocyanin (APC)-labelled Annexin V (Vazyme Biotech, China) and phycoerythrin (PE)-conjugated CD61 antibody (BD Biosciences, USA) for 30 minutes. As a negative control, a subpopulation of MPs was resuspended in Annexin V binding buffer lacking calcium and containing a PE-conjugated IgG control antibody. The MPs were then centrifuged at 20000 g for 30 minutes to remove excess fluorescent dye and washed twice by centrifugation for 30 minutes at 20 000 g. The pellet resuspended in 300 μl phosphate-buffered saline (PBS), followed the addition of 1×10^6 beads with a diameter of 3 μm. A tube containing beads with a diameter of 0.8 μm was used to gate the MPs. Finally, circulating PMPs were calculated by flow cytometry.

PMP isolation from activated platelets *in vitro*

Blood was collected from rats into centrifuge tubes with acid citrate dextrose (ACD) buffer. After resting for 10 minutes at room temperature, the blood was centrifuged at 282 g for 10 minutes at 22°C. The PRP was then centrifuged for 5 minutes at 400 g, and the supernatant was harvested and further centrifuged for 5 minutes at 1600 g to collect the platelets. After one wash of the pellet with citrate glucose saline (CGS) buffer, the platelets were resuspended in MTB. Platelets were counted and adjusted to a density of 3×10^8 cells/ml, followed by stimulation with 30 mmol/l of high glucose, 20 μg/ml of collagen(Type Ⅰ collagen, Sigma), or high glucose plus collagen for 30 minutes at 37°C. Ethylenediaminetetraacetic acid (20 mmol/l) was added to stop the platelet activation, and the residual platelets were removed by centrifuging twice for 5 minutes each at 2000 g. The supernatant was harvested and centrifuged for 90 minutes at 20000 g and 18°C to collect PMPs. Finally, the pellet containing the PMPs was resuspended in MTB. PMPs were stored at -80°C. To remove background dust and crystals, all reagents were double-filtered with 0.22-μm filters.

Protein microarray assay

Cytokines and chemokines in PMPs derived from platelets that were untreated or treated with collagen plus high glucose were measured using the Proteome Profiler™ (R&D, USA) according to the manufacturer's recommendations.

Histology and immunofluorescent staining

For histological analysis, tissues were dissected and fixed in 4% paraformaldehyde and

then embedded in paraffin. Sections were stained with periodic acid–Schiff (PAS) after deparaffinization. To evaluate the glomerular ESL glycocalyx, sections were stained with rhodamine-labelled wheat germ agglutinin (WGA) lectin (10 μg/ml) for 2 hours at room temperature after deparaffinization and analysed by Olympus fluorescence microscopy. For immunofluorescence, GEnCs and kidney sections were fixed with 4% paraformaldehyde for 30 minutes and treated with 0.05% Triton X-100 for 10 minutes. After blocking with 5% BSA, samples were stained with antibodies against CD61 (Novusbio, USA), CD63（Abcam, USA）, glypican-1, syndecan-1, CD31 (Santa Cruz, USA), and p-S6K1 (Abcam, USA). Secondary antibodies conjugated to Alexa Fluor 488, 555 or 594 were used (Life Technologies, USA). Nuclei were labelled with 4',6-diamidino-2-phenylindole. Coverslips were mounted on slides with glycerine and analysed by Olympus fluorescence microscopy. Fluorescent intensity analysis was performed with Image J.

PMPs internalization assay

Purified PMPs were labelled with PE-CD61 and incubated with GEnCs for 2, 4 or 12 hours. For uptake inhibition experiments, GEnCs were co-incubated with different inhibitors, as described in Figure. 2. Cells were fixed, permeabilized, and stained for CD31 with Alexa-Fluor-488 (Invitrogen， USA) and with the nuclear dye 4', 6-diamidino-2-phenylindole (DAPI). Imaging was performed on a fluorescence microscopy (Olympus, Japan) and fluorescent intensity analysis was performed with Image J.

The ultra-microstructure observation of PMPs

Rat kidneys were dissected and fixed in a mixture of 4% paraformaldehyde and 2.5% glutaraldehyde fixative buffered with PBS. After post-fixation with 0.4% OsO4, the samples were dehydrated with a graded series of acetone before embedding in Epon 812. After stained with uranyl acetate and lead citrate, the sections were observed with a JEM1230. The morphology of the isolated PMPs was determined using electron microscopy. PMPs pellets were fixed in 4% paraformaldehyde for 30 minutes. The pellets were then loaded on grids coated with formvar carbon and stained with 0.75% uranyl acetate. Sections were observed with a Philips Tecnai-10 transmission electron microscopy operating at 80 kilovolts (Phillips Electronic Instruments, USA). We further checked PMPs deposition in glomerular endothelial cells by immunoelectron microscopy assay. Brifely, 70 nm kidney sample sections were transferred to formvar-carbon coated copper grids. 1%H_2O_2 etching was used to remove osmium acid and then blocked with 5%BSA at room temperature for 60 minutes.The samples were then incubated with anti-CD61 antibody followed by secondary antibody conjugated with 10 nm gold. Finally, sections were observed with a Philips Tecnai-10 transmission electron microscopy.

Real-time polymerase chain reaction (PCR)

Total RNAs of GEnCs were extracted using TRIzol referring to the the manufacturer's instructions. The mRNA expression was detected by real-time PCR using the SYBR Green PCR Master Mix (Takara, Japan). The primer sequences are listed in

supplemental table 1.

Western blot analysis

Identical amounts of total protein extracts from renal cortex or cells were loaded and separated by 10% sodium dodecyl sulphate polyacrylamide gel electrophoresis, and the proteins were then transferred onto a nitrocellulose membrane. After treatment with blocking solution, the membranes were incubated with anti-rat antibodies against CD61, glypican-1, syndecan-1, ZO-1, occludin, CD31, mTOR, p-mTOR, S6K1, p-S6K1, 4EBP1, and p-4EBP1 overnight at 4°C, followed by horseradish peroxidase-conjugated secondary antibodies for two hours at 4℃. Finally, the results were determined using the ECL Advance system (Amersham Biosciences, USA).

Determination of ROS, NO, SOD, and eNOS

Cellular reactive oxygen species (ROS) were monitored as previously described. [30] Briefly, GEnCs were incubated with 10 μmol/l fluorescent probe DCFH-DA at 37°C for 30 minutes. After washing with PBS, the cells were harvested and resuspended in DMEM for flow cytometry. The nitric oxide (NO) levels in the renal cortex and cellular supernatant were measured using a commercially available NO assay kit. Nitric oxide synthase (NOS) activity in GEnCs was measured by detecting the conversion of l-[14C] arginine to l-[14C] citrulline using a commercial NOS Detect Assay kit. The anti-oxidative enzyme activity of superoxide dismutase (SOD) was measured using a commercial kit. The procedure was performed according to the manufacturer's

instructions.

GEnCs permeability assay

The permeability assay of the GEnCs was performed as previously described.[31] GEnCs were cultured in transwell plates. When cells in transwell membranes were fully confluent and formed an intact monolayer, the cells were treated for 24 hours. The cell culture medium was then removed, and 100 μl DMEM alone in the presence of fluorescein-isothiocyanate-labelled bovine serum albumin (FITC-BSA, 0.25 mg/ml) was added to the upper compartment. The medium of the lower compartment was collected after 60 minutes. FITC-BSA was quantified in a fluorescence spectrofluorophotometer. The BSA flux was valued as a ratio between fluorescence intensities in the lower compartment and the upper compartment.

Statistical analysis

Results are expressed as the mean±SD. Statistical analysis was performed using SPSS 16.0. Statistical comparisons among multiple groups were analysed for significance by one-way analysis of variance (ANOVA) followed by Tukey's or Games-Howell *post hoc* tests, or the Mann-Whitney U test for a nonparametric test. $P<0.05$ was considered a significant difference.

Results

Inhibition of PMPs decreased albuminuria and ameliorated glomerular

hypertrophy and mesangial matrix accumulation in early DN

We first determined whether PMPs were increased in a STZ-induced DM rat model. Circulating total MPs were isolated and detected by electron microscopy and flow cytometry assays. As shown in Figure 1A-B, vesicles from plasma ranged in size from 0.1 to 0.8 μm with clear intact double layer membrane structure. Using electron microscopy, we also found that DM rats produced more MPs than untreated controls. Treatment with aspirin significantly decreased MP formation at week 12(Figure 1B). To determine the plasma levels of PMPs, the specific marker CD61 of platelets with Annexin V were used to detect PMPs. Flow cytometry showed that the majority of these MPs were CD61 and Annexin V-positive PMPs, which gradually increased from week 4 to week 12 in diabetic rats compared with the controls (Figure 1C-D). Furthermore, by the end of week 12, the mean PMP count in the plasma of diabetic rats reached 20×10^6/ml (Figure 1D). Aspirin is one of the most commonly used anti-platelet agents and has potential effects on the prevention of platelet activation. The results showed that plasma levels of PMPs in diabetic rats treated with aspirin were significantly decreased starting from week 8 (Figure 1D). We further observed the PMPs infiltration in the glomeruli of rats. The results showed quantities of CD61-positive particles accumulated in the glomeruli of diabetic rats compared with the controls, suggesting that larger clusters of PMPs were deposited in the glomerulus (Figure 1E-F). In order to distinguish platelets and PMPs, kidney sections were incubated with freshly isolated platelets and stained with anti-CD61 antibody. The results showed the complete platelet structure in glomerulus and the PMPs were much smaller than the intact platelets

resided around the nuclei (supplemental Figure 2A). Double immunofluorescent staining showed that CD63, a biomarker for extracellular vesicle, overlapped with CD61 (Figure 1G). The co-localization confirmed that the CD61-positive structures represent PMPs. To further confirm that PMPs were internalized by glomerular endothelial cells, we ultrastructurally observed the deposition of PMPs in glomerular endothelial cells by immunoelectron microscopy assay. Results showed that there were quantities of CD61 positive dark black particles deposited in the cells, suggesting that PMPs were uptaked by glomerular endothelial cells (Supplemental Figure 2B). Moreover, Western blotting further demonstrated that CD61 protein expression was markedly upregulated in the kidneys of diabetic rats at week 12 (Figure 1H-I), suggesting that PMPs were incorporated into the glomerulus during the progression of DN. Interestingly, the deposition of PMPs in diabetic kidney was reduced after aspirin treatment (Figure 1E-F).

We then examined the role of the increased PMPs in the kidney injury of diabetic rats. Aspirin treatment did not affect the blood glucose levels of diabetic rats (Figure 1J). The results demonstrated no differences in serum creatinine in diabetic compared with control rats, although an increase in BUN was detected in diabetic rats from week 8 to week 12 (Figure 1K-L). Interestingly, inhibition of PMPs by aspirin was able to override the elevated urinary albumin/creatinine ratio (ACR) and kidney body weight ratio in diabetic rats (Figure 1M-N). PAS staining indicated that glomerular hypertrophy and mesangial matrix expansion in early DN were markedly ameliorated by aspirin treatment (Figure 1O-Q). Furthermore, after aspirin treatment, decreased plasma PMP

levels in diabetic rats were positively associated with a significant reduction of ACR (Figure 1R).

PMPs induced glomerular endothelial injury in early DN

As the glomerular endothelium directly contacts circulating PMPs, we checked the effects of PMPs on glomerular endothelial injury. Immunofluorescent staining showed that with an extended time of PMP co-incubation with GEnCs, endothelial cells showed increased PMP uptake (Figure 2A). To test whether PMPs were internalized by endothelial cells, we labelled PMPs with a R-phycoerythrin (PE)-tagged CD61 and co-incubated with GEnCs. High magnification pictures and the Z-section analysis indicated that most of the labelled PMPs were uptaken by GEnCs, and a few of them were combined on the membrane (Figure 2B, Supplemental Figure 7). To test whether uptake of PMPs into GEnCs was through endocytic pathways, we co-incubated GEnCs with PMPs alone or together with a series of known endocytosis inhibitors. Dynasore is an inhibitor of dynamin-2 required both for clathrin-mediated and caveolin-dependent endocytosis. Chlorpromazine, an inhibitor of clathrin-mediated endocytosis. We tested dynasore, chlorpromazine, the actin filament inhibitors - latrunculin A and cytochalasin D, and the microtubule inhibitors - nocodazole. We found that all these inhibitors had significant effects on PMPs uptake (Figure 2C-D), strongly suggesting that PMPs internalization by GEnCs is indeed via endocytosis.

The PMPs isolated from the plasma of diabetic rats decreased NO production and increased ROS levels in GEnCs in a dose-dependent manner (Figure 2E-F), indicating

that the PMPs from diabetic rats induced GEnCs dysfunction. To further confirm the effects of PMPs on endothelial injury, we isolated PMPs *in vitro* from cultured rat platelets activated with different agonists. The results demonstrated that the generation of PMPs from activated platelets stimulated by high glucose plus collagen (Col+HG-PMPs) was remarkably increased compared with high glucose (HG-PMPs) or collagen alone (Col-PMPs) (Figure 2G), suggesting that a high glucose background is a critical factor inducing and amplifying PMP generation in diabetes. A significant reduction of the NO levels was observed, with inhibition of eNOS and SOD activities, in contrast to increased production of ROS in GEnCs during stimulation with Col+HG-PMPs (Figure 2H-K). Consistently, immunofluorescence analysis confirmed that Col+HG-PMPs reduced the expression of glycocalyx-associated core proteins glypican-1 and syndecan-1 (Figure 2L). In addition, GEnC permeability was enhanced by Col+HG-PMPs, as shown by a significant increase in trans-endothelial FITC-BSA flux (Figure 2M).

The *in vivo* results revealed a gradually reduction of the ESL thickness, as assessed by rhodamine-WGA staining in diabetic rats compared with controls, which were reversed by aspirin (Figure 3A-B). Immunofluorescence and Western blot assays also revealed that expression levels of the glycocalyx-associated core proteins glypican-1 and syndecan-1 as well as the tight junction-associated protein ZO-1 and occludin in glomerular endothelium were downregulated in diabetic rats, whereas aspirin provided a protective role for the GEnC glycocalyx and tight junction in early DN (Figure 3C-H). Moreover, inhibition of PMPs by aspirin caused a reduction of ET-1 expression and

improvement of GEnC fenestration in diabetic rats (Figure 3G-K). To observe the effect of PMPs on GEnCs diastolic function, we detected the NO level and SOD activity in the kidney cortex. As shown in Figure 3L-M, the NO level and SOD activity were decreased in diabetic rats; however, this response was mitigated by aspirin treatment.

PMPs activated the mTORC1 pathway in GEnCs

We next investigated potential mechanisms of PMP-induced glomerular endothelial injury. The mTORC1 is a rapamycin-sensitive protein kinase complex that regulates processes of cell growth, metabolism, proliferation, and autophagy by phosphorylating p70 S6 kinase 1 (S6K1) and eukaryotic initiation factor 4E-binding protein 1 (4EBP1). Hyperactivation of mTORC1 in kidney cells is associated with early changes in DN. Although we did not observe a significant difference in mTOR, S6K1 and 4EBP1 at the mRNA level between the control and PMP-stimulated group (Figure 4A-C), immunofluorescent staining and Western blot analysis showed that PMPs significantly increased protein phosphorylation of mTOR, S6K1, and 4EBP1, indicating a hyperactivation of the mTORC1 pathway (Figure 4D-F). In the *in vivo* study, double immunofluorescent staining of p-S6K1 and CD31 showed that S6K1 phosphorylation was increased in the cytoplasm of CD31-positive cells in diabetic rats, suggesting an upregulation of mTORC1 activity in the glomerular endothelium(Figure 4G). Aspirin treatment prevented S6K1 phosphorylation in glomerular endothelial cells of diabetic rats (Figure 4G). Consistent with these findings, Western blot analysis also showed higher levels of p-mTOR, p-S6K1 and p-4EBP1 in the glomeruli of diabetic rats, which

were reversed by aspirin, confirming the contribution of PMPs to mTORC1 activation (Figure 4H-I).

PMPs mediated glomerular endothelial injury through activation of the mTORC1 pathway

To confirm whether mTORC1 signalling is involved in PMP-mediated glomerular endothelial injury, rapamycin or raptor siRNA was used to block this pathway. Western blotting showed that the increased protein expression of p-mTOR, p-S6K1 and p-4EBP1 in GEnCs was significantly inhibited by rapamycin or raptor-specific siRNA treatment (Figure 5A-B). Under these conditions, inhibition of mTORC1 reversed the PMP-induced decrease in NO levels and eNOS activity, and decreased ROS production (Figure 5C-E). Immunofluorescence and Western blot analysis indicated that rapamycin or raptor siRNA prevented PMP-induced upregulation of the ET-1 expression and downregulation of glypican-1, syndecan-1, ZO-1, and occludin (Figure 5F-H). Furthermore, inhibition of mTORC1 reversed the increased permeability of the glomerular endothelial cell barrier induced by PMP treatment (Figure 5I). To evaluate the role of mTORC1 signalling in glomerular endothelial injury of early DN, we treated diabetic rats with rapamycin. PMP deposition in the kidneys was not altered in rapamycin-treated compared with vehicle-treated diabetic rats (Figure 6A-B). As shown in Figure 6C-H, rapamycin prevented glomerular endothelial injury by improving the glomerular EC fenestration, ESL glycocalyx, and tight junctions, as well as by decreasing ET-1 expression. Moreover, rapamycin enhanced NO production and

SOD activity in the diabetic rats (Figure 6I-J).

PMP-derived CXCL7 promoted GEnCs damage

PMPs contain various pro-inflammatory and anti-inflammatory cytokines and chemokines deriving from platelets. PMPs can act as messengers and deliver these signals through soluble mediators, regulating lymphocyte rolling and activating endothelial cells, leukocytes and other platelets. Given the efficient uptake of PMPs by GEnCs (Figure 2B), we considered whether the binding of PMPs to GEnCs could deliver cytokines that target the mTORC1 signalling pathway. To characterize PMP-derived cytokines, PMP lysates were analysed with cytokine protein microarrays. We surveyed a range of cytokines elicited from activated PMPs and observed a large amount of the chemokine CXCL7 (Supplemental Figure 8A-B). For the following experiments, we focused on CXCL7 because this is the most abundant cytokine in PMPs. Consistently, CXCL7 expression was significantly higher in activated PMPs than normal PMPs by ELISA analysis (Figure 7A). Because CXCL7 mediates its effect through the G-protein-coupled receptors CXCR1 and CXCR2, we analysed the expression of CXCR1 and CXCR2 in PMPs treated GEnCs by RT-PCR. The results revealed higher expression of CXCR1 and CXCR2 in GEnCs that received activated PMPs treatment compared with those treated with normal PMPs (Figure 7B). Next, we sought to determine whether the abundant CXCL7 could recapitulate the effect on the GEnCs mTORC1 pathway of PMPs. Western blot analysis showed that CXCL7 increased the phosphorylation of mTORC1, S6K1 and 4EBP1 in GEnCs in a dose-

dependent manner (Figure 7C-D). However, SB225002, a competitive inhibitor of CXCR1 and CXCR2, reduced the PMP-induced mTORC1 activation in GEnCs (Figure 7E-F), indicating that CXCL7 is responsible for mTORC1 activation induced by PMPs in GEnCs.

To ascertain that CXCL7 mediated PMPs induced GEnCs damage, CXCR1/2 in GEnCs was antagonized by SB225002, and diastolic function, glycocalyx, cell junctions and permeability were analysed in GEnCs. We found that pretreatment with the SB225002 reversed the reduction of the NO level, eNOS and SOD activity, and decreased ROS production in GEnCs induced by PMPs (Figure 7G-J). Consistently, the destruction of the GEnC glycocalyx and cell junctions by PMPs was reversed by SB225002 (Figure 7K-N). Furthermore, blockade of CXCL7 by SB225002 preserved the permeability of the GEnCs barrier disrupted by PMPs (Figure 7O). Moreover, to test whether the PMPs-induced glomerular endothelial injury was dependent on CXCL7, CXCL7 blockade using CXCL7 neutralizing antibody was performed. Interestingly, anti-CXCL7 treatment led to a marked reduction of mTORC1 activity, increase of glycocalyx, and recovery of glomerular endothelium function under the stimulation of PMPs (Figure 8). These results indicated that CXCL7/CXCR1/2 pathway played a crucial role in the PMPs-induced glomerular endothelial injury.

Discussion

The release of PMPs after platelet activation is considered to be a novel effector that may play a key role in the development of diabetic nephropathy. Here we report that

PMPs participate in the intercellular communication between platelets and GEnCs via the delivery of platelet cytokines and regulation of protein expression, leading to glomerular endothelial injury and progression of early DN.

Our data showed that plasma PMPs level was significantly elevated in STZ-induced diabetic rats from week 4, and approximately 80% of circulating MPs were derived from platelets. This result was further confirmed in an *in vitro* study showing that high glucose effectively enhanced the ability of platelets to generate PMPs in the presence of agonists, suggesting that high glucose is a crucial contributor to the rise in PMP levels in diabetes. By immunofluorescence and Western blot analyses, we observed a large amount of accumulated PMPs in the glomeruli of diabetic rats, but rarely in the glomeruli of normal rats. This difference likely reflected alterations in the quantity and function of PMPs, and the abnormal glomerular endothelial activation in diabetes, favouring the aggregation of PMPs. Importantly, the significant increase in the PMP level in plasma and the glomerulus was inhibited by aspirin treatment, indicating that aspirin is a potential PMP inhibitor in diabetes. Furthermore, inhibition of PMPs by aspirin significantly ameliorated DN by reducing albuminuria, glomerular hypertrophy and mesangial matrix expansion, and it had no effect on blood glucose level. These results suggested a strong association between the increased PMP level and the progression of early DN.

Considering that the glomerular endothelium is in direct contact with blood and is vulnerable to PMPs, we then studied the effect of PMPs on the glomerular endothelium.

First, we demonstrated that most of plasma-derived PMPs from diabetic rats were uptaken by GEnCs when co-incubated *in vitro* and then PMPs were internalized by GEnCs via endocytosis in a variety of forms. The role of PMPs in diseases has recently begun to emerge and varies with different disease conditions and the different types of cells.[29, 32, 33] PMP stimulation *in vitro* induced tumour cell apoptosis,[34] inhibited regulatory T cell production of IL-17,[35] and induced fibroblast-like synoviocytes to release IL-8.[36] Our results indicated that plasma PMPs led directly to the decrease in NO synthase activity and increase in ROS production in GEnCs. Therefore, we further investigated the effect of PMPs on GEnCs by using purified PMPs derived from activated platelets stimulated by agonists *in vitro*. Consistently, PMPs released from activated platelets effectively inhibited NO synthase activity and SOD production, but increased ROS production, in GEnCs. In addition, PMPs reduced expression of the glycocalyx-associated core proteins glypican-1 and syndecan-1, suggesting a disruption of GEnC structural integrity. The permeability assay confirmed that PMPs reduced permeability of the glomerular endothelial cell barrier, as shown by increased FITC-BSA passage through GEnCs. These alterations of GEnCs induced by PMPs are consistent with the manifestations of glomerular endothelium injury in DN. To confirm these findings from the *in vitro* study, we treated diabetic rats with aspirin, which effectively reduced the level of PMPs from week 8. Consistently, our *in vivo* study revealed that inhibition of PMPs protected against GEnC injury in early DN, favouring the restoration of GEnC fenestration, improvement of the glycocalyx and tight junctions, and increased NO synthesis and SOD activity. A previous clinical study reported that

the circulating PMP level was associated with micro- and macro-angiopathy in young patients with type 1 diabetes. [23] Here, we first demonstrated that PMPs contributed to the progression of early DN by directly inducing glomerular endothelial damage. It suggests that PMPs could be a therapeutic target for the treatment of early DN. Tarnow *et al*. found that nephropathy in type 1 diabetes was associated with increased circulating activated platelets and platelet hyperreactivity[37]. Some clinical and experimental studies reported that aspirin provided a renoprotective role in DN, which was mainly through reducing urinary protein, decreasing the expression of inflammatory factors and collagen in kidneys[38, 39]. However, clinical application of aspirin in DN treatment is still relatively insufficient and its mechanism for DN improvement is not very clear. Our findings evoked a novel therapeutic concept for DN, implying that the pharmacological inhibition of PMPs released from activated platelets might prevent glomerular endothelial injury. Thus, besides traditional pharmacological efficacies, aspirin could be exploited as a drug for the prevention of glomerular endothelial injury in the progression of early DN.

Next, we explored potential mechanisms of glomerular endothelial injury induced by PMPs. It has been reported that PMPs regulate the signalling pathway in target cells both at the gene and protein levels depending on its contents. Ceroi *et al* [40] demonstrated that PMPs stimulated liver X receptor activation in plasmacytoid dendritic cells. Laffont *et al* [34] showed that PMPs regulated the gene expression of F-box/WD repeat-containing protein 7 and ephrin A1 in human umbilical vein endothelial cells. Increasing evidence has indicated that mTORC1 plays a crucial role in the regulation

of kidney cell homeostasis and has been implicated in the development of glomerular lesions in DN.[41] The activation of mTORC1 induces oxidative stress, apoptosis, and phenotypic changes in podocytes.[42, 43] In addition, downregulation of the mTORC1 pathway alleviates hindlimb ischaemic injury in diabetic mice by improving the vascular structure as well as attenuating the inflammation, oxidative stress, and apoptosis in endothelial cells.[44] Our previous studies indicated that mTORC1 activation induced by inflammation contributed to atherosclerosis through disruption of the low-density lipoprotein receptor pathway in vascular smooth muscle cells.[45] In the present study, we demonstrated that PMPs activated the mTORC1 pathway by increasing the phosphorylation levels of mTOR and their downstream proteins S6K1 and 4EBP1 in GEnCs *in vitro*. In contrast, inhibition of PMPs by aspirin decreased activation of the mTORC1 pathway in GEnCs of diabetic rats. Disruption of mTORC1 signalling by the knockdown of raptor or rapamycin protected against the PMP-induced decrease in NO synthases, SOD and eNOS activity, increase of ROS production, loss of glycocalyx and tight junctions, and hyperpermeability in GEnCs. Consistent with these *in vitro* results, rapamycin improved the above alterations of GEnCs in early DN, although the PMP level in kidney was not changed. Thus, the mTORC1 pathway modulated PMP-induced GEnC injury.

It is known that PMPs are the basic storage units for different active proteins in platelets, including resting platelet membrane proteins and a variety of active substances. Previous studies have verified the capacity of PMPs to elicit or disseminate a range of cytokines and chemokines, transcription factors, and microRNAs to recipient cells.[34, 46]

For example, Michael *et al* [47] showed that PMPs infiltrated solid tumours and transferred platelet RNA to tumour cells *in vivo* and *in vitro*. Using a protein microarray technique, we found that activated platelets released the vast majority of inflammatory cytokines in PMPs. CXCL7 was richly expressed and significantly increased in PMPs released by activated platelets. CXCL7 is one kind of cytokine in the CXCL family that signal through the G-protein-coupled receptors CXCR1 and CXCR2, which leads to activation of intracellular signalling pathways.[48] In this study, we found that the expression of CXCR1 and 2 in GEnCs significantly increased following treatment with PMPs, suggesting that PMP-derived CXCL7 interacted with GEnCs by binding to CXCR1 and 2. Interestingly, CXCL7 activated the mTORC1 pathway in GEnCs in a dose-dependent manner, which was inhibited by CXCL7 blockade using CXCL7 neutralizing antibody or an inhibitor of CXCL7 receptors, SB225002. These findings suggest that CXCL7 is a major PMP-derived regulator of glomerular endothelial injury.

In summary, increased PMPs contributed to glomerular endothelial injury in early DN through the CXCL7 released from PMPs. The potential underlying mechanism was correlated with activation of the mTORC1 pathway in glomerular endothelial cells induced by CXCL7. Persistent PMP release finally resulted in functional and structural damage to the glomerular endothelium, an increase in permeability, urinary albumin leakage, and the progression of DN (Figure 9). Our findings herein may provide a potential drug therapeutic target for the prevention of early DN onset and progression.

Author contributions

K.L.M. planned the study and designed the experiments. Y. Z. performed most of the experiments. G.H.W, Z.B.H, and L.L. helped to perform animal experiments. J.L. helped to isolate circulating PMPs. C.P.P and L.C.C helped to culture the GEnCs. Y.Z. and K.L.M wrote the manuscript. B.C.L. and X.Z.R. help to modify the manuscript.

Acknowledgements

This work was supported by the National Natural Science Foundation of China (grant 81470957), the Jiangsu Province Social Development Project (BE2018744), the Project for Jiangsu Provincial Medical Talent (ZDRCA2016077), the Jiangsu Province Six Talent Peaks Project (2015-WSN-002), the Scientific Research Foundation of Graduate School of Southeast University (YBJJ1640), the Fundamental Research Funds for the Central Universities (KYCX18-0182, KYCX17-0169, KYZZ15-0061), the Jiangsu Province Ordinary University Graduate Research Innovation Project (SJZZ16-004), the Natural Science Foundation of Jiangsu Province (BK20141343), the Project of Nanjing Municipal Committee for Health and Family Planning (YKK17280), and Major Program of National Natural Science Foundation of China (81720108007).

Disclosures

None.

Supplemental contents Supplemental table1 and Supplemental Figure 1-8.

References

1. Flyvbjerg A: The role of the complement system in diabetic nephropathy. *Nat*

Rev Nephrol 13:311-318, 2017.

2. Olshansky SJ, Passaro DJ, Hershow RC, Layden J, Carnes BA, Brody J, *et al*: A potential decline in life expectancy in the united states in the 21st century. *N Engl J Med* 352:1138-1145, 2005.

3. Tirosh A, Shai I, Tekes-Manova D, Israeli E, Pereg D, Shochat T, *et al*:. Normal fasting plasma glucose levels and type 2 diabetes in young men. *N Engl J Med* 353:1454-1462, 2005.

4. Haase VH: A breath of fresh air for diabetic nephropathy. *J Am Soc Nephrol* 26:239-24, 2015.

5. Satchell SC, Tooke JE: What is the mechanism of microalbuminuria in diabetes: A role for the glomerular endothelium? *Diabetologia* 51:714-725, 2008.

6. Satchell SC: The glomerular endothelium emerges as a key player in diabetic nephropathy. *Kidney Int* 82:949-95, 2012.

7. Satchell S: The role of the glomerular endothelium in albumin handling. *Nat Rev Nephrol* 9:717-725, 2013.

8. Haraldsson B, Nystrom J: The glomerular endothelium: New insights on function and structure. *Curr Opin Nephrol Hypertens* 21:258-263, 2012.

9. Obeidat M, Obeidat M, Ballermann BJ: Glomerular endothelium: A porous sieve and formidable barrier. *Exp Cell Res* 318:964-972, 2012.

10. Wu D, Yang X, Zheng T, Xing S, Wang J, Chi J, *et al*: A novel mechanism of action for salidroside to alleviate diabetic albuminuria: Effects on albumin transcytosis across glomerular endothelial cells. *Am J Physiol Endocrinol*

Metab 310:E225-237, 2016.

11. Salmon AH, Ferguson JK, Burford JL, Gevorgyan H, Nakano D, Harper SJ, *et al*: Loss of the endothelial glycocalyx links albuminuria and vascular dysfunction. *J Am Soc Nephrol* 23:1339-1350, 2012.
12. Friden V, Oveland E, Tenstad O, Ebefors K, Nystrom J, Nilsson UA, *et al*: The glomerular endothelial cell coat is essential for glomerular filtration. *Kidney Int* 79:1322-1330, 2011.
13. Kuwabara A, Satoh M, Tomita N, Sasaki T, Kashihara N: Deterioration of glomerular endothelial surface layer induced by oxidative stress is implicated in altered permeability of macromolecules in zucker fatty rats. *Diabetologia* 53:2056-2065, 2010.
14. Takahashi T, Harris RC: Role of endothelial nitric oxide synthase in diabetic nephropathy: Lessons from diabetic enos knockout mice. *J Diabetes Res* 2014:590541, 2014.
15. Nakagawa T, Sato W, Glushakova O, Heinig M, Clarke T, Campbell-Thompson M, *et al*: Diabetic endothelial nitric oxide synthase knockout mice develop advanced diabetic nephropathy. *J Am Soc Nephrol* 18:539-550, 2007.
16. Burnouf T, Goubran HA, Chou ML, Devos D, Radosevic M: Platelet microparticles: Detection and assessment of their paradoxical functional roles in disease and regenerative medicine. *Blood Rev* 28:155-166, 2014.
17. Italiano JE, Jr., Mairuhu AT, Flaumenhaft R: Clinical relevance of microparticles from platelets and megakaryocytes. *Curr Opin Hematol* 17:578-

584, 2010.

18. Milioli M, Ibanez-Vea M, Sidoli S, Palmisano G, Careri M, Larsen MR: Quantitative proteomics analysis of platelet-derived microparticles reveals distinct protein signatures when stimulated by different physiological agonists. *J Proteomics* 121:56-66, 2015.

19. Akbiyik F, Ray DM, Gettings KF, Blumberg N, Francis CW, Phipps RP: Human bone marrow megakaryocytes and platelets express ppargamma, and ppargamma agonists blunt platelet release of cd40 ligand and thromboxanes. *Blood* 104:1361-1368, 2004.

20. Spinelli SL, Casey AE, Pollock SJ, Gertz JM, McMillan DH, Narasipura SD, *et al*: Platelets and megakaryocytes contain functional nuclear factor-kappab. *Arterioscler Thromb Vasc Biol* 30:591-598, 2010.

21. Lannan KL, Sahler J, Kim N, Spinelli SL, Maggirwar SB, Garraud O, *et al*: Breaking the mold: Transcription factors in the anucleate platelet and platelet-derived microparticles. *Front Immunol* 6:48, 2015.

22. Barry OP, Pratico D, Savani RC, FitzGerald GA: Modulation of monocyte-endothelial cell interactions by platelet microparticles. J Clin Invest 102:136-144, 1998.

23. Salem MA, Adly AA, Ismail EA, Darwish YW, Kamel HA: Platelets microparticles as a link between micro- and macro-angiopathy in young patients with type 1 diabetes. *Platelets* 26:682-688, 2015.

24. Tokarz A, Szuscik I, Kusnierz-Cabala B, Kapusta M, Konkolewska M,

Zurakowski A, *et al*: Extracellular vesicles participate in the transport of cytokines and angiogenic factors in diabetic patients with ocular complications. *Folia Med Cracov* 55:35-48, 2015.

25. Zhang X, McGeoch SC, Megson IL, MacRury SM, Johnstone AM, Abraham P, *et al*. Oat-enriched diet reduces inflammatory status assessed by circulating cell-derived microparticle concentrations in type 2 diabetes. *Mol Nutr Food Res* 58:1322-1332, 2014.

26. Zhang X, McGeoch SC, Johnstone AM, Holtrop G, Sneddon AA, MacRury SM, *et al*: Platelet-derived microparticle count and surface molecule expression differ between subjects with and without type 2 diabetes, independently of obesity status. *J Thromb Thrombolysis* 37:455-463, 2014.

27. Tesch GH, Allen TJ: Rodent models of streptozotocin-induced diabetic nephropathy. *Nephrology* 12:261-266,2007.

28. Fang J, Wang M, Zhang W, Wang Y: Effects of dexamethasone on angiotensin ii-induced changes of monolayer permeability and f-actin distribution in glomerular endothelial cells. *Exp Ther Med* 6:1131-1136, 2013.

29. Dasgupta SK, Le A, Chavakis T, Rumbaut RE, Thiagarajan P: Developmental endothelial locus-1 (del-1) mediates clearance of platelet microparticles by the endothelium. *Circulation* 125:1664-1672, 2012.

30. Wu X, Deng G, Li M, Li Y, Ma C, Wang Y, *et al*: Wnt/beta-catenin signaling reduces bacillus calmette-guerin-induced macrophage necrosis through a ros -mediated parp/aif-dependent pathway. *BMC Immunol* 16:16, 2015.

31. Kiemer AK, Weber NC, Furst R, Bildner N, Kulhanek-Heinze S, Vollmar AM: Inhibition of p38 mapk activation via induction of mkp-1: Atrial natriuretic peptide reduces tnf-alpha-induced actin polymerization and endothelial permeability. *Circ Res* 90:874-881, 2002.

32. Faille D, Combes V, Mitchell AJ, Fontaine A, Juhan-Vague I, Alessi MC *et al*: Platelet microparticles: A new player in malaria parasite cytoadherence to human brain endothelium. *FASEB J* 23:3449-3458, 2009.

33. Faille D, El-Assaad F, Mitchell AJ, Alessi MC, Chimini G, Fusai T, *et al*: Endocytosis and intracellular processing of platelet microparticles by brain endothelial cells. *J Cell Mol Med* 16:1731-1738, 2012.

34. Laffont B, Corduan A, Ple H, Duchez AC, Cloutier N, Boilard E, *et al*: Activated platelets can deliver mrna regulatory ago2*microrna complexes to endothelial cells via microparticles. *Blood* 122:253-261, 2013.

35. Dinkla S, van Cranenbroek B, van der Heijden WA, He X, Wallbrecher R, Dumitriu IE, *et al*: Platelet microparticles inhibit il-17 production by regulatory t cells through p-selectin. *Blood* 127:1976-1986, 2016.

36. Boilard E, Nigrovic PA, Larabee K, Watts GF, Coblyn JS, Weinblatt ME, *et al*: Platelets amplify inflammation in arthritis via collagen-dependent microparticle production. *Science* 327:580-583, 2010.

37. Tarnow I, Michelson AD, Barnard MR, Frelinger AL, 3rd, Aasted B, Jensen BR, *et al*: Nephropathy in type 1 diabetes is associated with increased circulating activated platelets and platelet hyperreactivity. *Platelets*. 20:513-519, 2009.

38. Khajehdehi P, Roozbeh J, Mostafavi H. A comparative randomized and placebo-controlled short-term trial of aspirin and dipyridamole for overt type-2 diabetic nephropathy. *Scand J Urol Nephrol* 36:145-148, 2002.

39. Donadio JV Jr, Ilstrup DM, Holley KE Romero JC: Platelet-inhibitor treatment of diabetic nephropathy: a 10-year prospective study. *Mayo Clin Proc* 63(1):3-15, 1988.

40. Ceroi A, Delettre FA, Marotel C, Gauthier T, Asgarova A, Biichle S, *et al*: The anti-inflammatory effects of platelet-derived microparticles in human plasmacytoid dendritic cells involve liver x receptor activation. *Haematologica* 101:e72-76, 2016.

41. Fantus D, Rogers NM, Grahammer F, Huber TB, Thomson AW: Roles of mtor complexes in the kidney: Implications for renal disease and transplantation. *Nat Rev Nephrol* 12:587-609, 2016.

42. Inoki K, Mori H, Wang J, Suzuki T, Hong S, Yoshida S, *et al*: Mtorc1 activation in podocytes is a critical step in the development of diabetic nephropathy in mice. *J Clin Invest* 121:2181-2196, 2011.

43. Godel M, Hartleben B, Herbach N, Liu S, Zschiedrich S, Lu S, *et al*: Role of mtor in podocyte function and diabetic nephropathy in humans and mice. *J Clin Invest* 121:2197-2209, 2011.

44. Fan W, Han D, Sun Z, Ma S, Gao L, Chen J, *et al*: Endothelial deletion of mtorc1 protects against hindlimb ischemia in diabetic mice via activation of autophagy, attenuation of oxidative stress and alleviation of inflammation. *Free Radic Biol*

Med 108:725-740, 2017.

45. Ma KL, Liu J, Wang CX, Ni J, Zhang Y, Wu Y, *et al*: Activation of mtor modulates srebp-2 to induce foam cell formation through increased retinoblastoma protein phosphorylation. *Cardiovasc Res* 100:450-460, 2013.

46. Jiang J, Kao CY, Papoutsakis ET: How do megakaryocytic microparticles target and deliver cargo to alter the fate of hematopoietic stem cells? *J Control Release 10:*247:1-18, 2017.

47. Michael JV, Wurtzel JGT, Mao GF, Rao AK, Kolpakov MA, Sabri A, *et al*: Platelet microparticles infiltrating solid tumors transfer mirnas that suppress tumor growth. *Blood* 130:567-580, 2017.

48. Grepin R, Guyot M, Giuliano S, Boncompagni M, Ambrosetti D, Chamorey E, *et al*: The cxcl7/cxcr1/2 axis is a key driver in the growth of clear cell renal cell carcinoma. *Cancer Res* 74:873-883, 2014.

Figure legends

Fig. 1. Inhibition of PMPs decreased albuminuria and ameliorated glomerular hypertrophy and mesangial matrix accumulation in early DN. Diabetes was induced by one intraperitoneal injection of STZ at 60 mg/kg body weight in 0.1 mol/l of sodium citrate buffer. Normal control rats were treated with vehicle (Ctrl) and diabetic rats were treated with vehicle (DM) or aspirin (15 mg/kg) (DM+Asp), and then killed at weeks 4, 8, and 12. (A-B) Plasma MPs were isolated according to a circulating MP isolation procedure and observed by electron microscopy (scale bar: 200nm and

500nm). (C) The plasma PMP level was analysed by flow cytometry. MPs from DM rats or annexin V buffer controls, isotype controls， and MPs after lysis were analysed by flow cytometry. PMPs were defined as CD61+/Annexin V+ events in Q2 window and analysed for quantification. (D) The results are expressed as events/ml of plasma (mean±SD, n=8). *P<0.05, **P<0.01 compared with Ctrl; $^{\#}P$<0.05 compared with DM group. (E-F) The presence of $CD61^{+}$ PMPs (green dots) within the glomeruli in the renal cortexes of rats at week 12 was determined by immunofluorescent staining. Nuclei were stained with DAPI (blue). (scale bar: 20 μm). (G) Double immunofluorescent staining of CD61 (green) and CD63 (red) in glomeruli of DM rats at week 12. Nuclei were stained with DAPI (blue). (scale bar: 20 μm). (H and I) Protein levels of CD61 in renal cortexes of rats at week 12 were detected by Western blotting. The relative density of protein bands were quantified and normalized to β-actin (mean±SD, n=5). *P<0.05, **P<0.01 compared with Ctrl; $^{\#}P$< 0.05 compared with DM group. Blood glucose levels (J), BUN (K), serum creatinine (L), the urinary albumin/creatinine ratio (M), and the ratio of kidney weight to body weight (N) in rats were measured (mean±SD, n=8). *P<0.05, **P<0.01 compared with Ctrl; $^{\#}P$<0.05 and $^{\#\#}P$<0.01 compared with DM group. (O) Histopathological changes were evaluated by PAS staining. Original magnification, ×400 (scale bar: 50μm). (P-Q) The glomerular area and mesangial expansion score were determined from histology sections. *P<0.05, **P<0.01 compared with Ctrl; $^{\#}P$<0.05 and ##P<0.01 compared with DM group. (Q) Correlation analysis between the plasma PMP level and urinary albumin/creatinine ratio was determined by Spearman’s rank-order correlation analysis.

Fig. 2. PMPs induced glomerular endothelial injury *in vitro*. (A-B) Primary GEnCs were incubated with diabetic rat-derived PMPs labelled with PE-conjugated anti-CD61 (red) antibody for 0, 2, 4, and 12 hours at 37°C. The GEnCs were labelled with Alexa 488-conjugated anti-CD31 (green) antibody and nuclei were stained with DAPI (blue), and uptake of PMPs was observed by confocal microscopy (scale bars: 20 μm and 10μm). (C-D). GEnCs were co-incubated with PMPs labelled by PE-CD61 and inhibitors for 4 hours, PMPs uptake was quantified compared with control. The results were expressed as mean number of PMPs per cell. Ctrl: control. Dyn: Dynasore (80 μmol/l). Chlo: Chlorpromazine (10 μg/ml). Lat: Latrunculin A (5 μmol/l) .Cyto: Cytochalasin D (600 nmol/l). Noco: Nocodazole (20 μmol/l). (scale bars: 5μm). (E and F) Primary GEnCs were incubated without or with 0, 10^3/ml, 10^4/ml, 10^5/ml, and 10^6/ml of MPs derived from diabetic rats for 24 hours. The NO level in the culture supernatant (E) and intracellular ROS in GEnCs (F) were measured (mean±SD, n=4 experiments). **P*<0.05 compared with control (Ctrl); ***P*<0.05 compared with DM-PMPs (10^3), ****P*<0.05 compared with DM-PMPs (10^4), *****P*<0.05 compared with DM-PMPs (10^5). (G) PMPs were isolated from platelets stimulated without or with collagen (Col, 25 μg/ml), high glucose (HG, 30 mmol/l), or collagen plus high glucose (Col+HG) and quantified by flow cytometry. The results are expressed as the mean fold changes *vs* unstimulated platelets, which were used as a reference (mean±SD, n=3 experiments). **P*<0.05, ***P*<0.01 compared with Ctrl; $^{\#}$*P*<0.05 compared with Col-PMPs group. (H-K) Primary GEnCs were incubated without or with 5×10^6 /ml of different types of PMPs for 24 hours. NO level (H) in culture supernatant, activity of eNOS (I) and SOD (J),

and intracellular ROS (K) were measured in GEnCs (mean±SD, n=3 experiments). *P<0.05, **P<0.01 compared with Ctrl; $^{\#}P$<0.05 compared with Col-PMPs group. (L) Expression of glypican-1 (green) and syndecan-1 (red) in GEnCs was determined by immunofluorescent staining. Nuclei were stained with DAPI (blue) (scale bars: 20 μm). (M) The permeability of GEnCs was assessed by measuring the ratio of FITC-labelled albumin in the bottom after 1 hour (mean±SD, n=4 experiments).*P< 0.05, **P<0.01 compared with Ctrl; $^{\#}P$<0.05 compared with Col-PMPs group.

Fig. 3. Inhibition of PMPs protected glomerular endothelium against injury in early DN. Diabetes was induced by one intraperitoneal injection of STZ at 60 mg/kg body weight in 0.1 mol/l of sodium citrate buffer. Normal control rats were treated with vehicle (Ctrl) and diabetic rats were treated with vehicle (DM) or aspirin (15 mg/kg) (DM+Asp), and then killed at weeks 4, 8, and 12. (A) Glomerular ESL was determined by staining with rhodamine-labelled WGA. A coat of glomerular endothelial glycocalyx lined the luminal surface of the endothelial cells. Original magnification, ×400(scale bars: 20 μm); enlarged image magnification, ×800(scale bars: 5 μm).(B) Quantitation of WGA staining in the glomerulus. *P<0.05, **P<0.01 compared with Ctrl; $^{\#}P$<0.05, $^{\#\#}P$<0.01 compared with DM. (C and D) The expression of glypican-1 (green) and syndecan-1 (red) in renal tissues of rats was determined by immunofluorescent staining. Original magnification, ×400 (scale bars: 20 μm). (E and F) Quantitation of immunofluorescent staining for glypican-1 and syndecan-1. *P<0.05, **P<0.01 compared with Ctrl; $^{\#}P$<0.05, $^{\#\#}P$<0.01 compared with DM. (G-H) Protein levels of glypican-1, syndecan-1, ZO-1, occludin, and ET-1 in renal cortexes of rats

were detected by Western blotting. The relative density of the protein bands was quantified and normalized to β-actin (mean±SD, n=5). *P<0.05, **P<0.01 compared with Ctrl; $^{\#}P$<0.05, $^{\#\#}P$<0.01 compared with DM. (I) The ultra-microstructure of the glomerular filtration barrier, including the endothelial fenestration, glomerular basement membrane, and podocyte foot processes, was analysed by transmission electron microscopy (scale bars: 0.5 μm).(J-K) The glomerular endothelial fenestration and glomerular basement membrane thickness were determined from ultra-microstructure images. *P<0.05, **P<0.01 compared with Ctrl; $^{\#}P$<0.05, $^{\#\#}P$<0.01 compared with DM group. (L) NO level and (M) SOD activity in the renal cortex of rats were measured (mean±SD; n=5). *P<0.05, **P<0.01 compared with Ctrl; $^{\#}P$<0.05, $^{\#\#}P$<0.01 compared with DM group.

Fig. 4. PMP activation of mTORC1 signalling in GEnCs. (A-F) Primary GEnCs were incubated without or with 5×10^6 /ml of different types of PMPs for 24 hours. (A-C) mRNA level of mTOR, S6K1 and 4EBP1 in GEnCs was detected by real-time PCR. (D) Expression of p-S6K1 in GEnCs was detected by immunofluorescent staining. Original magnification, ×400. (Scale bars: 20 μm). (E-F) Protein levels of mTOR, p-mTOR, S6K1, p-S6K1, 4EBP1 and p-4EBP1 in GEnCs were detected by Western blotting. The relative intensity of protein bands was quantified, and the ratio of phosphoprotein to total protein was expressed (mean±SD, n=3 experiments). *P<0.05, **P<0.01 compared with Ctrl. (G-I) Diabetes was induced by one intraperitoneal injection of STZ at 60 mg/kg body weight in 0.1 mol/l of sodium citrate buffer. Normal control rats were treated with vehicle (Ctrl) and diabetic rats were treated with vehicle

(DM) or aspirin (15 mg/kg) (DM+Asp) for 12 weeks. (G) Co-expression of p-S6K1 and CD31 in renal tissues of rats was determined by immunofluorescent staining. Original magnification, ×400 (scale bars: 20 μm). (H-I) Protein levels of mTOR, p-mTOR, S6K1, p-S6K1, 4EBP1 and p-4EBP1 in renal cortexes of rats were detected by Western blotting. The relative intensity of protein bands was quantified, and the ratio of phosphoprotein to total protein was expressed (mean±SD, n=5). **P*<0.05, ***P*<0.01 compared with Ctrl; $^{\#}P$<0.05, $^{\#\#}P$<0.01 compared with DM group.

Fig. 5. PMPs mediated glomerular endothelial injury through activation of the mTORC1 pathway *in vitro*. Primary GEnCs were incubated without (Ctrl) or with 5×10^6 /ml of PMPs (PMPs), PMPs plus 10 ng/ml of rapamycin (PMPs+Rapa), or pretreated with raptor siRNA (PMPs+siRaptor) or negative control siRNA (PMPs+siCtrl) for 24 hours. (A-B) Protein levels of mTOR, p-mTOR, S6K1, p-S6K1, 4EBP1 and p-4EBP1 in GEnCs were detected by Western blotting. The relative intensity of the protein bands was quantified, and the ratio of phosphoprotein to total protein was expressed (mean±SD, n=3 experiments). **P*<0.05, ***P*<0.01 compared with Ctrl; $^{\#}P$<0.05, $^{\#\#}P$<0.01 compared with PMPs group. The NO level (C), eNOS activity (D), and intracellular ROS (E) in GEnCs were measured (mean±SD, n=3 experiments). **P*<0.05, ***P*<0.01 compared with Ctrl; $^{\#}P$<0.05, $^{\#\#}P$<0.01 compared with PMPs group. (F) The expression of glypican-1 (green) and syndecan-1 (red) in GEnCs was determined by immunofluorescent staining. Nuclei were stained with DAPI (blue). Original magnification, ×400 (scale bars: 20 μm). (G-H) Protein levels of glypican-1, syndecan-1, ZO-1, occludin, and ET-1 in renal cortexes of rats were

detected by Western blotting. The relative intensity of the protein bands was quantified and normalized to β-actin (mean±SD, n=3 experiments). *P< 0.05, **P<0.01 compared with Ctrl; $^{\#}P$<0.05, $^{\#\#}P$<0.01 compared with PMPs group. (I) The permeability of GEnCs was assessed by measuring the ratio of FITC-labelled albumin in the bottom after 1 hour (mean±SD, n=4 experiments). *P< 0.05, **P< 0.01 compared with Ctrl; $^{\#}P$< 0.05, $^{\#\#}P$<0.01 compared with PMPs group.

Fig. 6. PMPs mediated glomerular endothelial injury through activation of the mTORC1 pathway *in vivo*. Diabetes was induced by one intraperitoneal injection of STZ at 60 mg/kg body weight in 0.1 mol/l of sodium citrate buffer. Normal control rats were treated with vehicle (Ctrl) and diabetic rats were treated with vehicle (DM) or rapamycin (1 mg/kg) (DM+Rapa), and then killed at week 12. (A-B) The presence of $CD61^{+}$ PMPs (green dots) within the glomerulus in the renal cortexes of rats was detected by immunofluorescent staining followed by fluorescence semi-quantitative analysis. Nuclei were stained with DAPI (blue) (scale bar: 20 μm). (mean±SD, n=5). *P<0.05, **P<0.01 compared with Ctrl. (C-D) The ultra-microstructure of endothelial fenestration was observed by electron microscopy and the endothelial fenestrations were quantified. (scale bars: 0.5 μm). *P<0.05, **P<0.01 compared with Ctrl; $^{\#}P$<0.05 compared with DM. (E) Glomerular ESL was determined by staining with rhodamine-labelled WGA. A coat of glomerular endothelial glycocalyx lined the luminal surface of endothelial cells. Original magnification, ×400(scale bars: 20 μm); enlarged image magnification, ×800(scale bars: 5 μm). (F) Expression of glypican-1 (green) and syndecan-1 (red) in renal tissues of rats was determined by immunofluorescent staining.

Original magnification, ×400 (scale bars: 20 μm). Nuclei were stained with DAPI (blue). (G and H) Protein levels of glypican-1, syndecan-1, ZO-1, occludin, and ET-1 in renal cortexes of rats were detected by Western blotting. The relative intensity of the protein bands was quantified and normalized to β-actin (mean±SD, n=5). *P<0.05, **P<0.01 compared with Ctrl; $^{\#}P$<0.05, $^{\#\#}P$<0.01 compared with DM. (I) NO levels and SOD activity (J) in renal cortexes of rats were measured (mean±SD, n=5). *P<0.05, **P<0.01 compared with Ctrl; $^{\#}P$<0.05, $^{\#\#}P$<0.01 compared with DM.

Fig. 7. PMP-derived CXCL7 contributed to GEnC injury. (A) Concentrations of CXCL7 in different types of PMPs lysate were measured by ELISA (mean±SD, n=4 experiments). *P<0.05, **P<0.01 compared with Ctrl. (B) Primary GEnCs were incubated with Ctrl or Col+HG-PMPs for 24 hours. The mRNA levels of the CXCR1 and CXCR2 in GEnCs were determined by real-time PCR (mean±SD, n=3 experiments). *P<0.05, **P<0.01 compared with Ctrl. (C-D) GEnCs were treated with CXCL7 (1, 10, 20, 40 or 100 ng/ml) for 24 hours. Protein levels of mTOR, p-mTOR, S6K1, p-S6K1, 4EBP1 and p-4EBP1 in GEnCs were detected by Western blotting. The relative intensity of the protein bands was quantified, and the ratio of phosphoprotein to total protein was expressed (mean±SD, n=3 experiments). *P<0.05, **P<0.01 compared with Ctrl.(E-O) GEnCs were pretreated without or with SB225002 (1 mmol/l) for 2 hours and then incubated with 5×10^6/ml PMPs for 24 hours. (E-F) Protein levels of mTOR, p-mTOR, S6K1, p-S6K1, 4EBP1 and p-4EBP1 in GEnCs were detected by Western blotting. The relative intensity of the protein bands was quantified, and the ratio of phosphoprotein to total protein was expressed (mean±SD, n=3 experiments).

*P<0.05, **P<0.01 compared with Ctrl; $^{\#}P$< 0.05, $^{\#\#}P$<0.01 compared with PMPs. NO level (G), eNOS (H) and SOD (I) activity, and and intracellular ROS (J) in GEnCs were measured (mean±SD, n=4 experiments). *P<0.05, **P<0.01 compared with Ctrl; $^{\#}P$<0.05, $^{\#\#}P$<0.01 compared with PMPs. (K) The GEnC glycocalyx was evaluated by WGA staining. (scale bars: 20 μm) (L) Expression of glypican-1 (green) and syndecan-1 (red) in GEnCs was determined by immunofluorescent staining. Nuclei were stained with DAPI (blue). Original magnification, ×400 (scale bars: 20 μm). (M-N) Protein levels of glypican-1, syndecan-1, ZO-1, occludin, and ET-1 in renal cortexes of rats were detected by Western blotting. The relative intensity of the protein bands was quantified and normalized to β-actin (mean±SD, n=3 experiments). *P<0.05, **P<0.01 compared with Ctrl; $^{\#}P$<0.05, $^{\#\#}P$<0.01 compared with PMPs. (O) Permeability of GEnCs was assessed by measuring the ratio of FITC-labelled albumin in the bottom after one hour (mean±SD, n=4 experiments). *P<0.05, **P<0.01 compared with Ctrl; $^{\#}P$<0.05, $^{\#\#}P$ <0.01 compared with PMPs.

Fig. 8. CXCL7 neutralizing antibody blocked PMP-derived CXCL7 induced GEnC injury. GEnCs were treated with 5×10^6/ml PMPs for 24 hours and anti-rat CXCL7 antibodies(1 μg/ml) for 24 hours. (A-B) Protein levels of mTOR, p-mTOR, S6K1, p-S6K1, 4EBP1 and p-4EBP1 in GEnCs were detected by Western blotting. The relative intensity of the protein bands was quantified, and the ratio of phosphoprotein to total protein was expressed (mean±SD, n=3 experiments). *P<0.05, **P<0.01 compared with Ctrl; #P< 0.05, ##P<0.01 compared with PMPs. NO level (C), eNOS (D) and SOD (E) activity in GEnCs were measured (mean±SD, n=4 experiments).

*P<0.05, **P<0.01 compared with Ctrl; $^{\#}P$<0.05, $^{\#\#}P$<0.01 compared with PMPs. (F) The GEnC glycocalyx was evaluated by immunofluorescent staining of glypican-1 (green) and syndecan-1 (red) and WGA staining. Nuclei were stained with DAPI (blue). Original magnification, ×400 (scale bars: 10 μm)**.**

Fig. 9 Schematic diagram showing the role and mechanism of PMPs in glomerular endothelial injury in early diabetic nephropathy (DN). (A). In early DN, circulating PMPs released from activated platelets under hyperglycaemia conditions infiltrated the glomerulus and bound to the glomerular endothelium, thereby promoting glomerular endothelial injury and albumin leakage.(B) PMP-derived CXCL7 induced a reduction of the NO levels and eNOS and SOD activities, production of ROS in GEnCs, and destruction of GEnC glycocalyx and cell junctions, and hyperpermeability in GEnCs by activating the mTORC1 pathway.

Figure 1

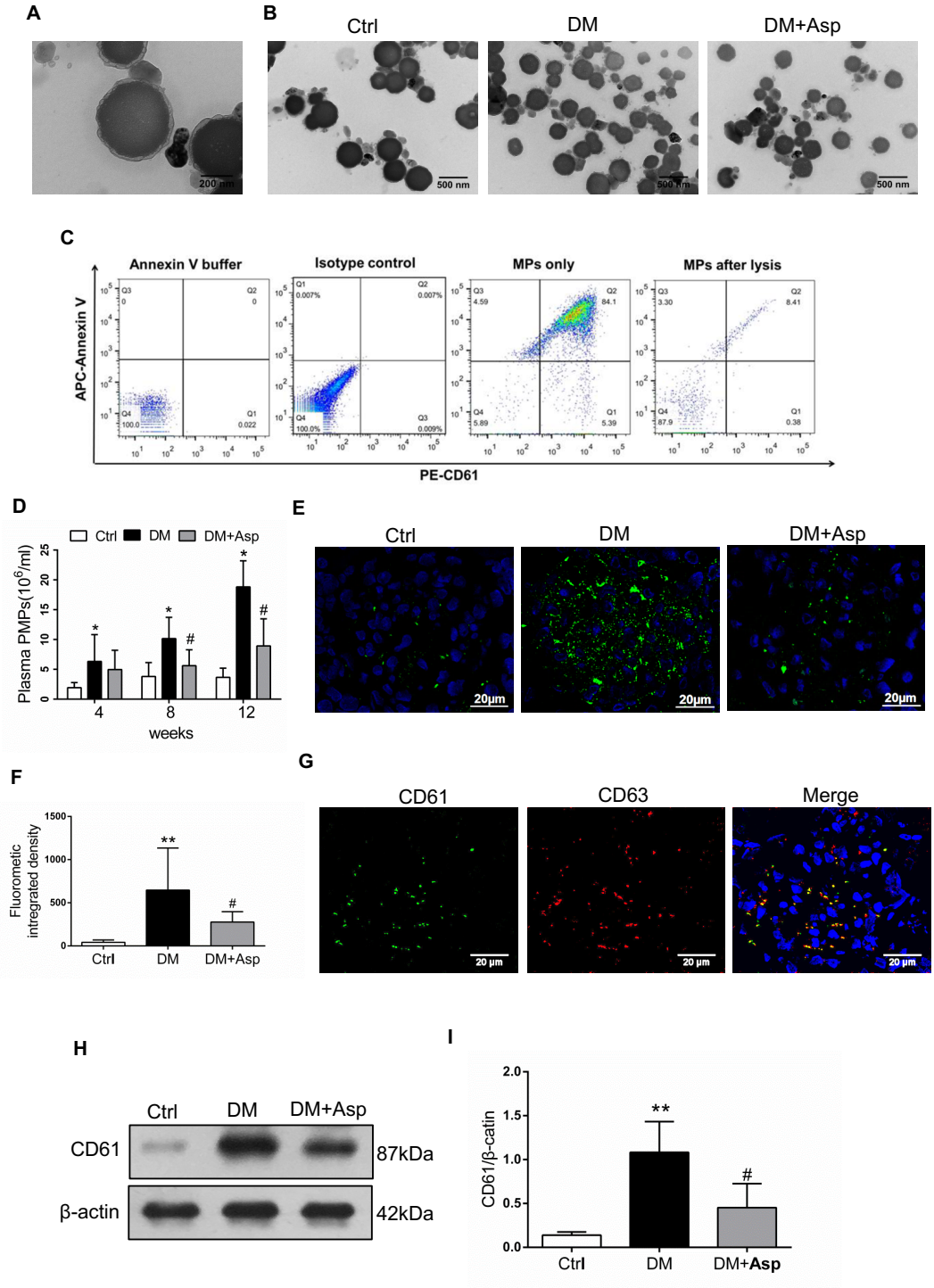
A
B
Ctrl
DM
DM+Asp
200 nm
500 nm
C
Annexin V buffer
Isotype control
MPs only
MPs after lysis
APC-Annexin V
PE-CD61
D
Ctrl DM DM+Asp
Plasma PMPs(10^6/ml)
weeks
E
Ctrl
DM
DM+Asp
20μm
F
Fluorometic intregrated density
G
CD61
CD63
Merge
20 μm
H
Ctrl DM DM+Asp
CD61
β-actin
87kDa
42kDa
I
CD61/β-catin
Ctrl
DM
DM+Asp

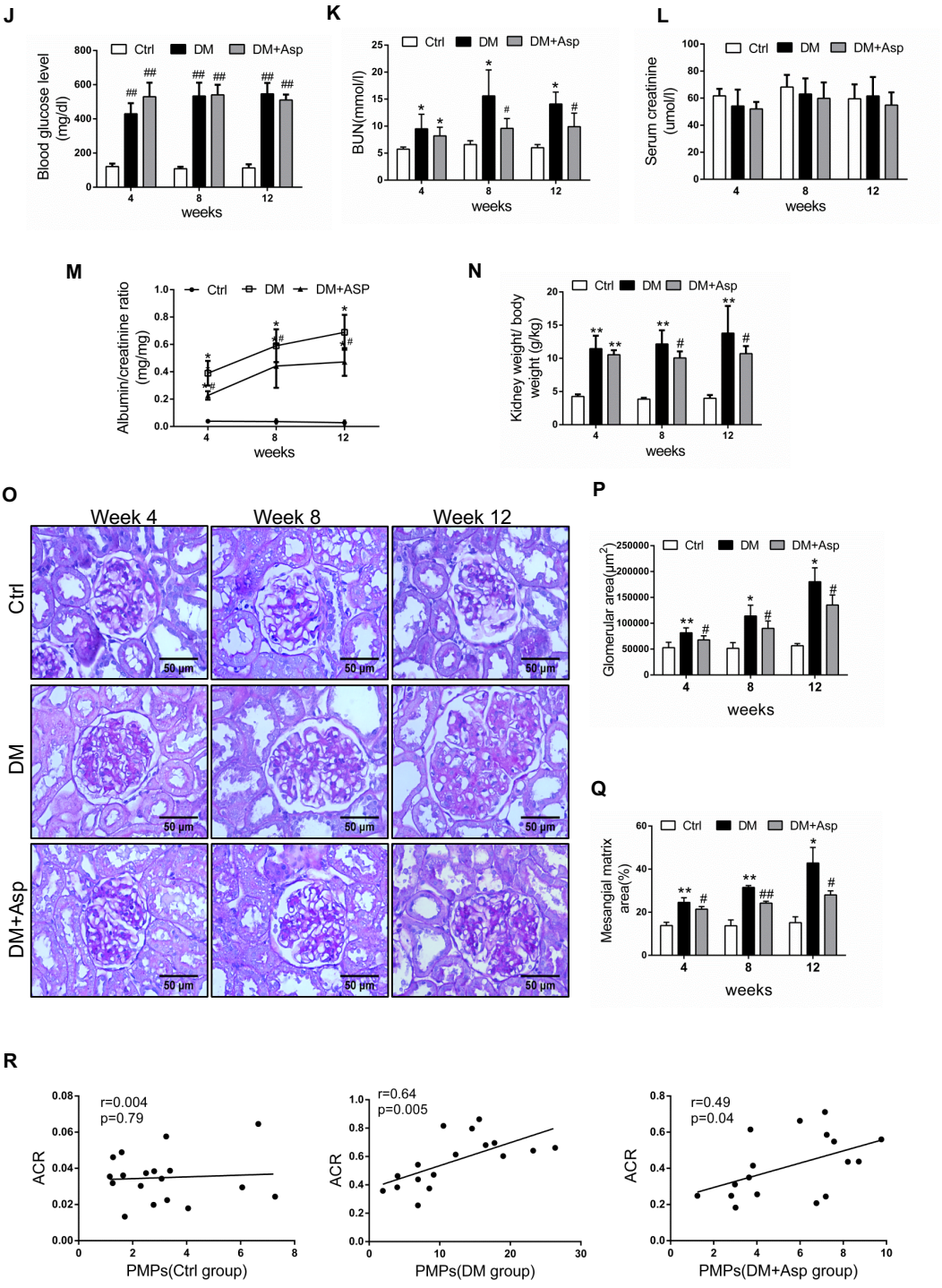
J
Blood glucose level (mg/dl)
Ctrl
DM
DM+Asp
weeks
K
BUN(mmol/l)
L
Serum creatinine (umol/l)
M
Albumin/creatinine ratio (mg/mg)
DM+ASP
N
Kidney weight/ body weight (g/kg)
O
Week 4
Week 8
Week 12
Ctrl
DM
DM+Asp
50 μm
P
Glomerular area(μm2)
Q
Mesangial matrix area(%)
R
ACR
r=0.004
p=0.79
PMPs(Ctrl group)
r=0.64
p=0.005
PMPs(DM group)
r=0.49
p=0.04
PMPs(DM+Asp group)

Figure 2

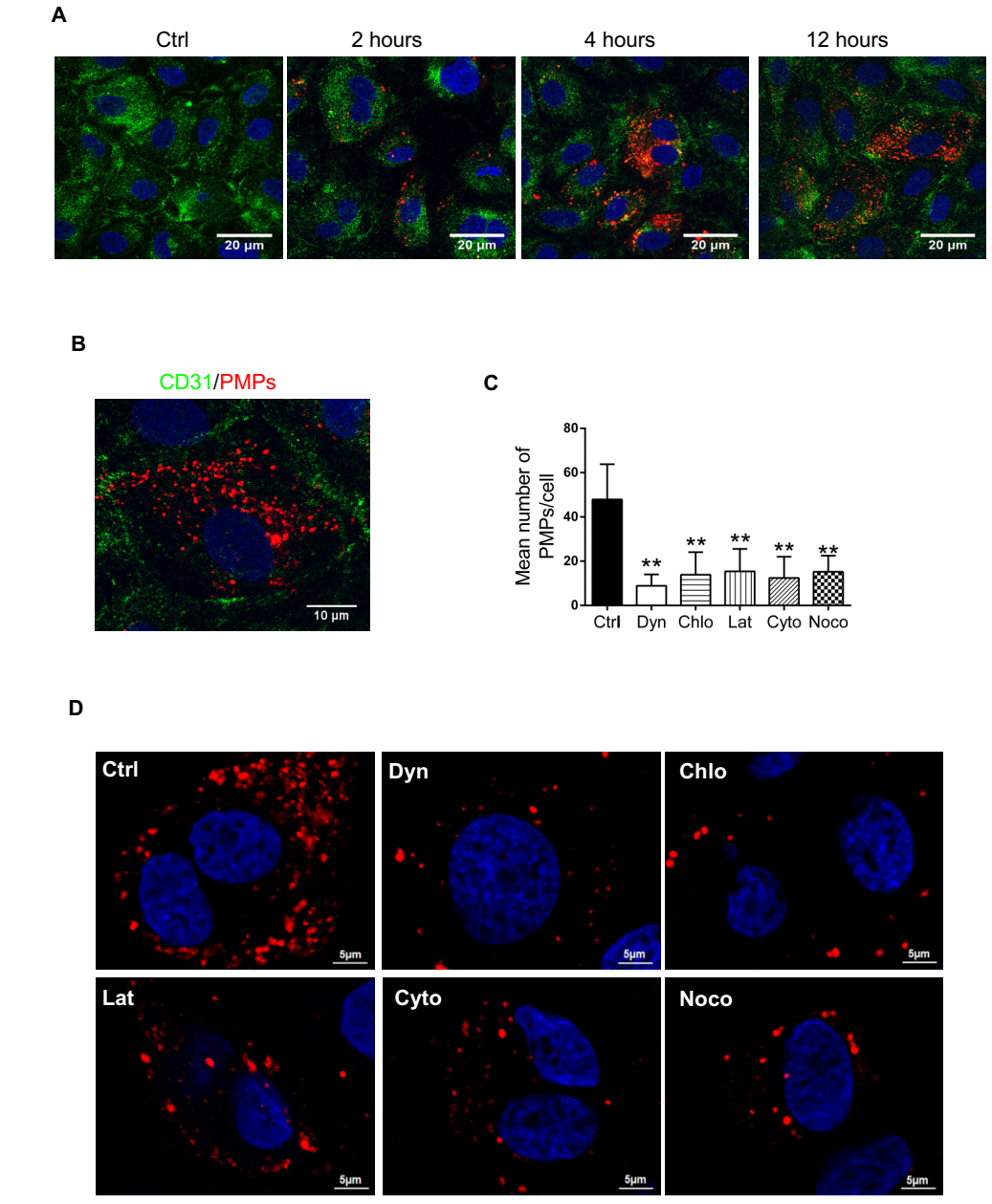
A
Ctrl
2 hours
4 hours
12 hours
20 µm
B
CD31/PMPs
10 µm
C
Mean number of PMPs/cell
80
60
40
20
0
**
Ctrl
Dyn
Chlo
Lat
Cyto
Noco
D
Ctrl
Dyn
Chlo
Lat
Cyto
Noco
5µm

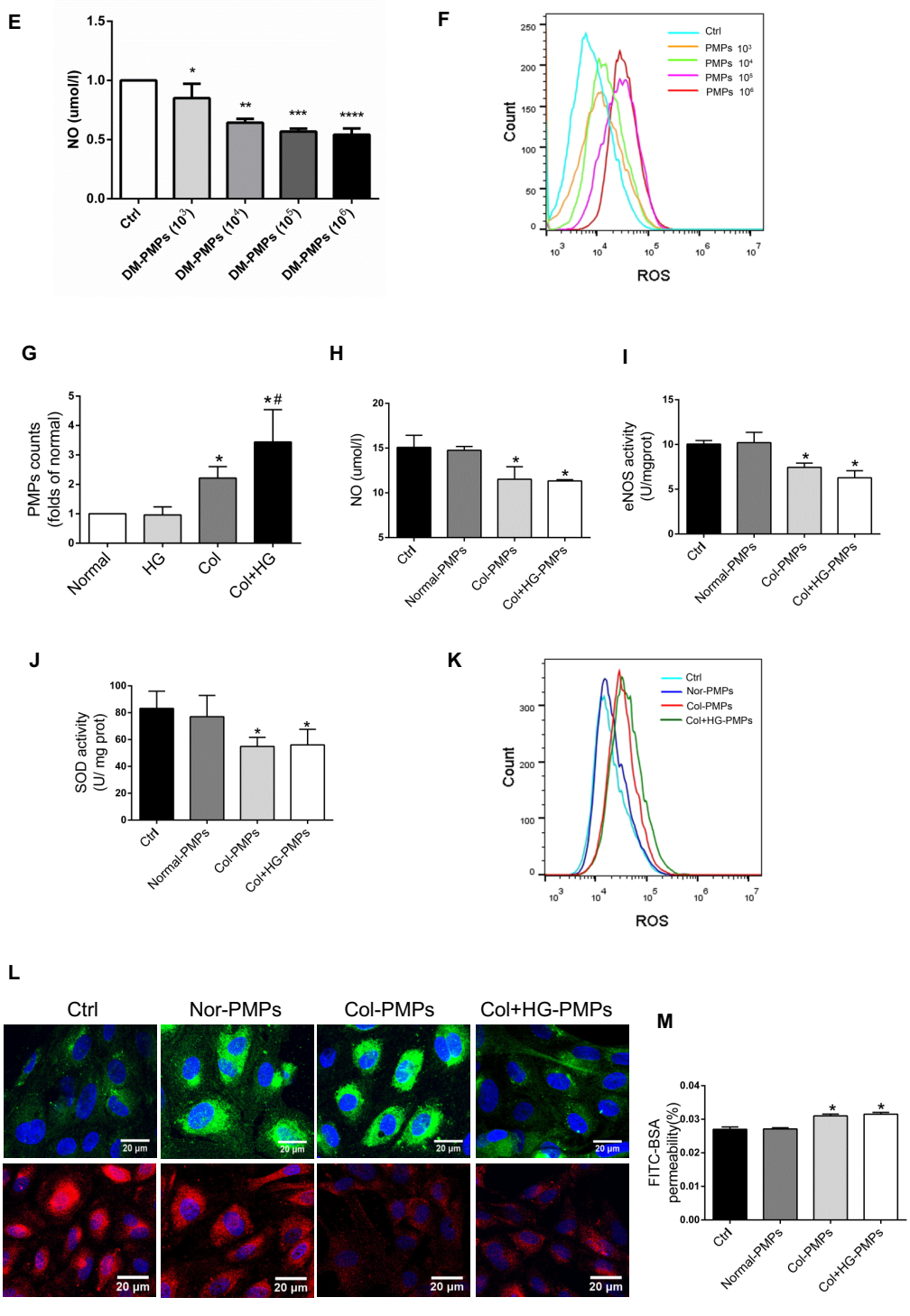
E
NO (umol/l)
Ctrl
DM-PMPs (10^3)
DM-PMPs (10^4)
DM-PMPs (10^5)
DM-PMPs (10^6)
F
Count
ROS
Ctrl
PMPs 10^3
PMPs 10^4
PMPs 10^5
PMPs 10^6
G
PMPs counts (folds of normal)
Normal
HG
Col
Col+HG
H
NO (umol/l)
I
eNOS activity (U/mgprot)
Ctrl
Normal-PMPs
Col-PMPs
Col+HG-PMPs
J
SOD activity (U/ mg prot)
K
Nor-PMPs
L
Nor-PMPs
M
FITC-BSA permeability(%)
20 μm

Figure 3

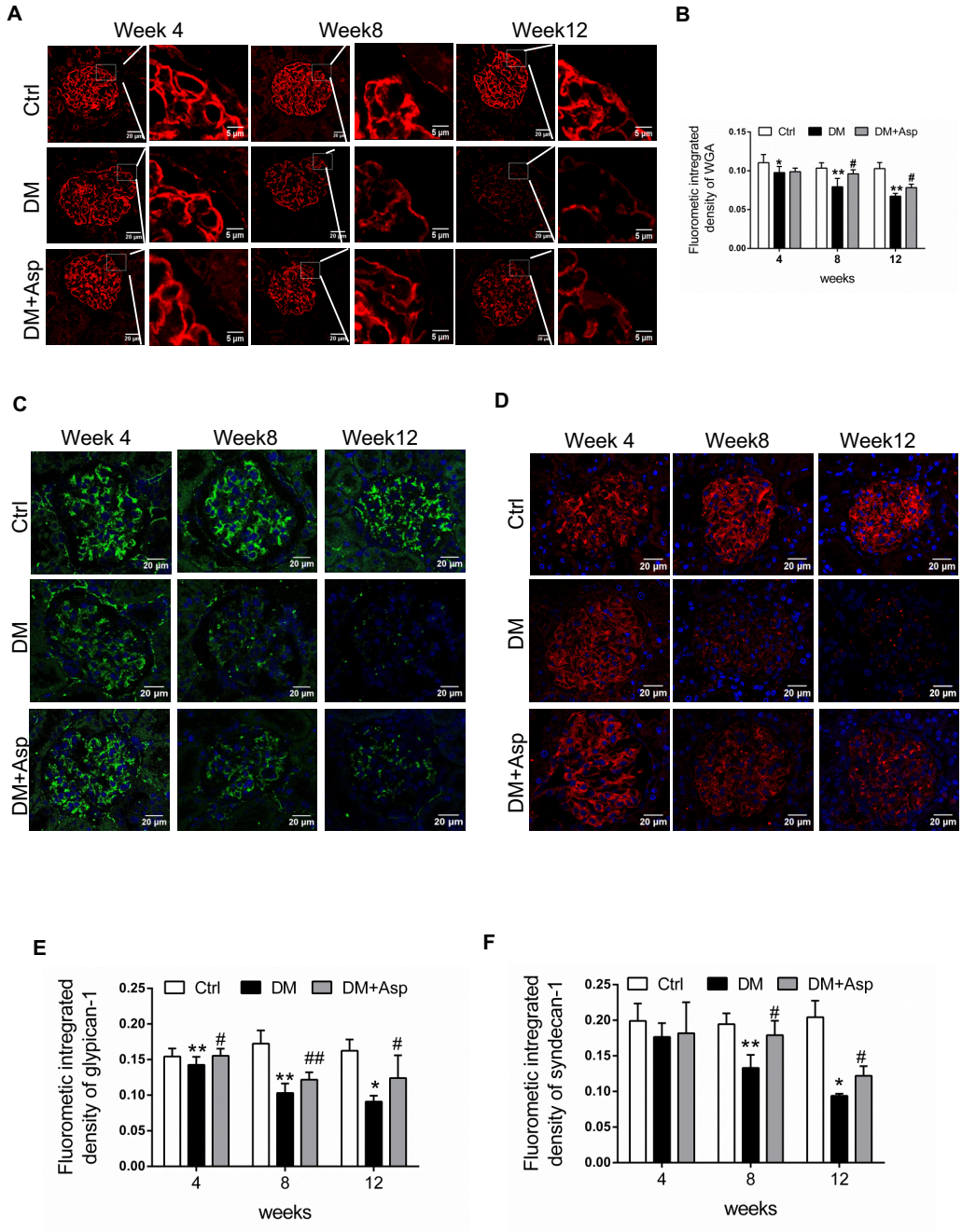
A
Week 4
Week8
Week12
Ctrl
DM
DM+Asp
B
Fluorometic intregrated density of WGA
Ctrl
DM
DM+Asp
weeks
C
Week 4
Week8
Week12
Ctrl
DM
DM+Asp
D
Week 4
Week8
Week12
Ctrl
DM
DM+Asp
E
Fluorometic intregrated density of glypican-1
Ctrl
DM
DM+Asp
weeks
F
Fluorometic intregrated density of syndecan-1
Ctrl
DM
DM+Asp
weeks

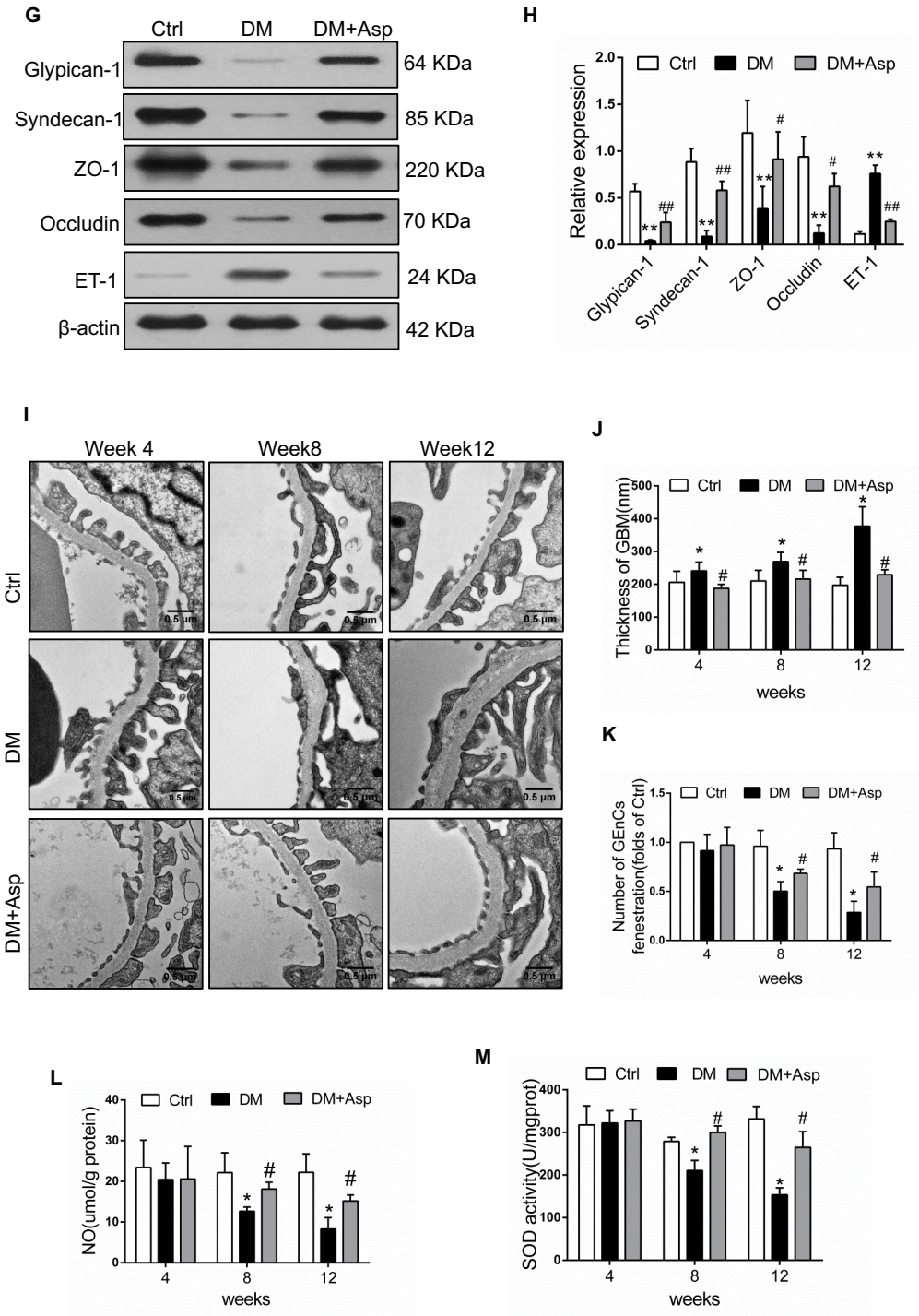
G
Ctrl
DM
DM+Asp
Glypican-1
Syndecan-1
ZO-1
Occludin
ET-1
β-actin
64 KDa
85 KDa
220 KDa
70 KDa
24 KDa
42 KDa
H
Relative expression
Ctrl
DM
DM+Asp
Glypican-1
Syndecan-1
ZO-1
Occludin
ET-1
I
Week 4
Week8
Week12
Ctrl
DM
DM+Asp
0.5 μm
J
Thickness of GBM(nm)
weeks
K
Number of GEnCs fenestration(folds of Ctrl)
weeks
L
NO(umol/g protein)
weeks
M
SOD activity(U/mgprot)
weeks

Figure 4

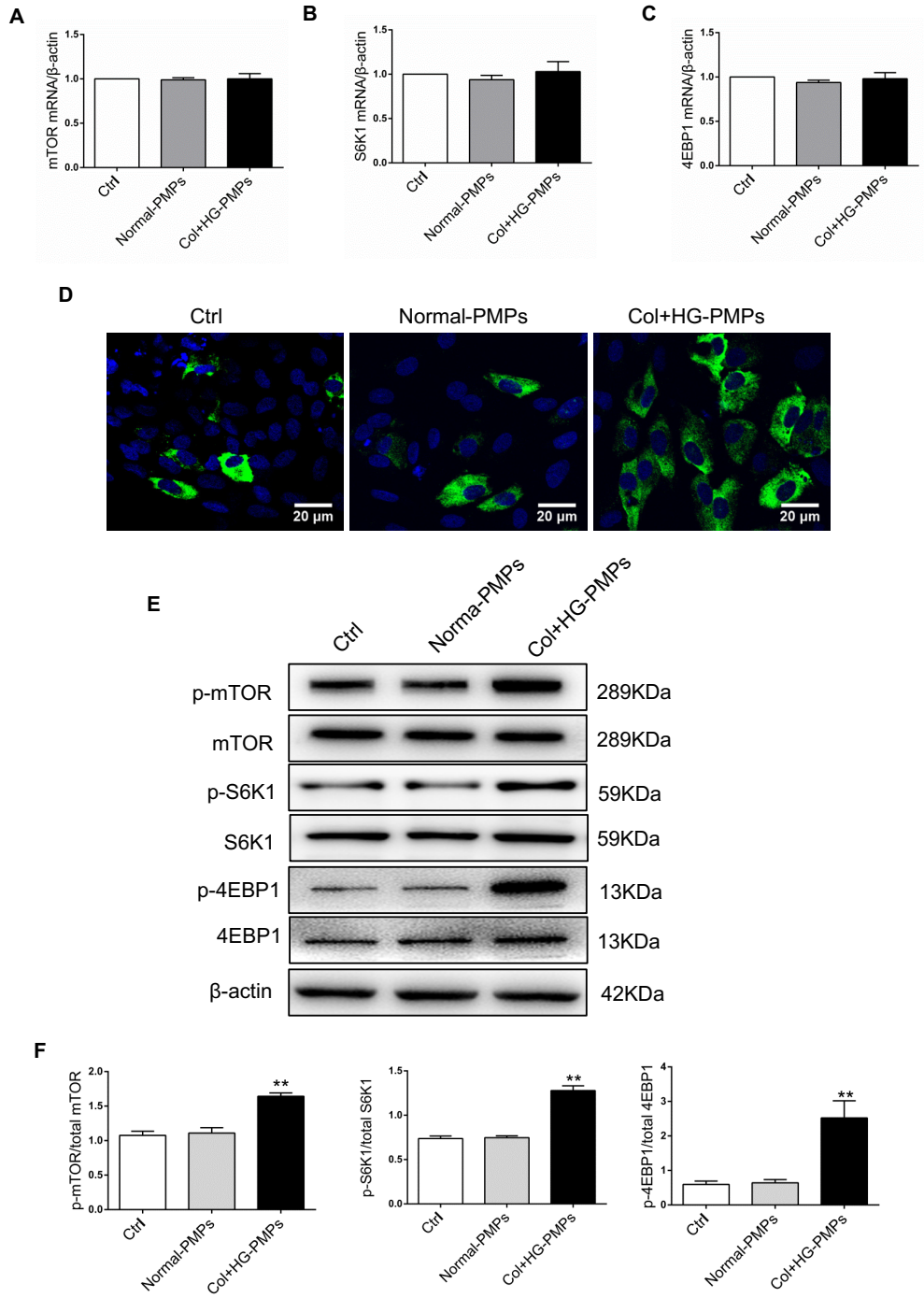
A
mTOR mRNA/β-actin
Ctrl
Normal-PMPs
Col+HG-PMPs
B
S6K1 mRNA/β-actin
C
4EBP1 mRNA/β-actin
D
Ctrl
Normal-PMPs
Col+HG-PMPs
20 μm
E
Ctrl
Norma-PMPs
Col+HG-PMPs
p-mTOR
289KDa
mTOR
289KDa
p-S6K1
59KDa
S6K1
59KDa
p-4EBP1
13KDa
4EBP1
13KDa
β-actin
42KDa
F
p-mTOR/total mTOR
p-S6K1/total S6K1
p-4EBP1/total 4EBP1
**

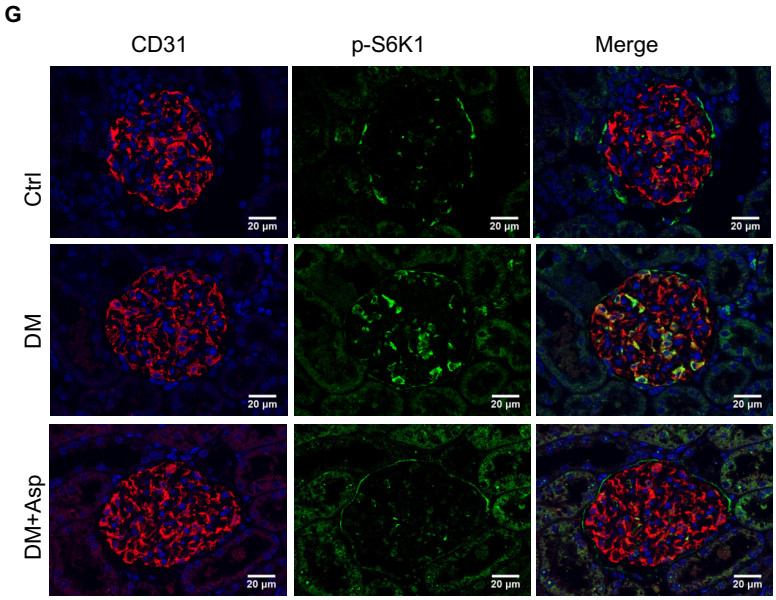
G
CD31
p-S6K1
Merge
Ctrl
DM
DM+Asp
20 μm

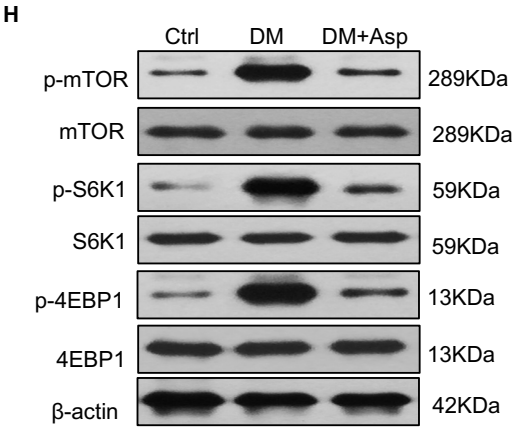
H
Ctrl
DM
DM+Asp
p-mTOR
289KDa
mTOR
289KDa
p-S6K1
59KDa
S6K1
59KDa
p-4EBP1
13KDa
4EBP1
13KDa
β-actin
42KDa

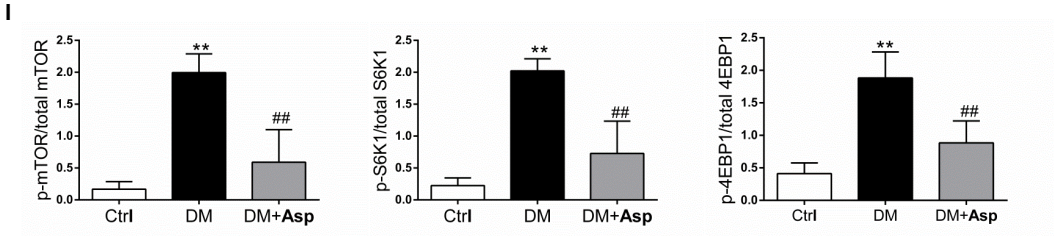
I
p-mTOR/total mTOR
p-S6K1/total S6K1
p-4EBP1/total 4EBP1
**
##
Ctrl
DM
DM+Asp

Figure 5

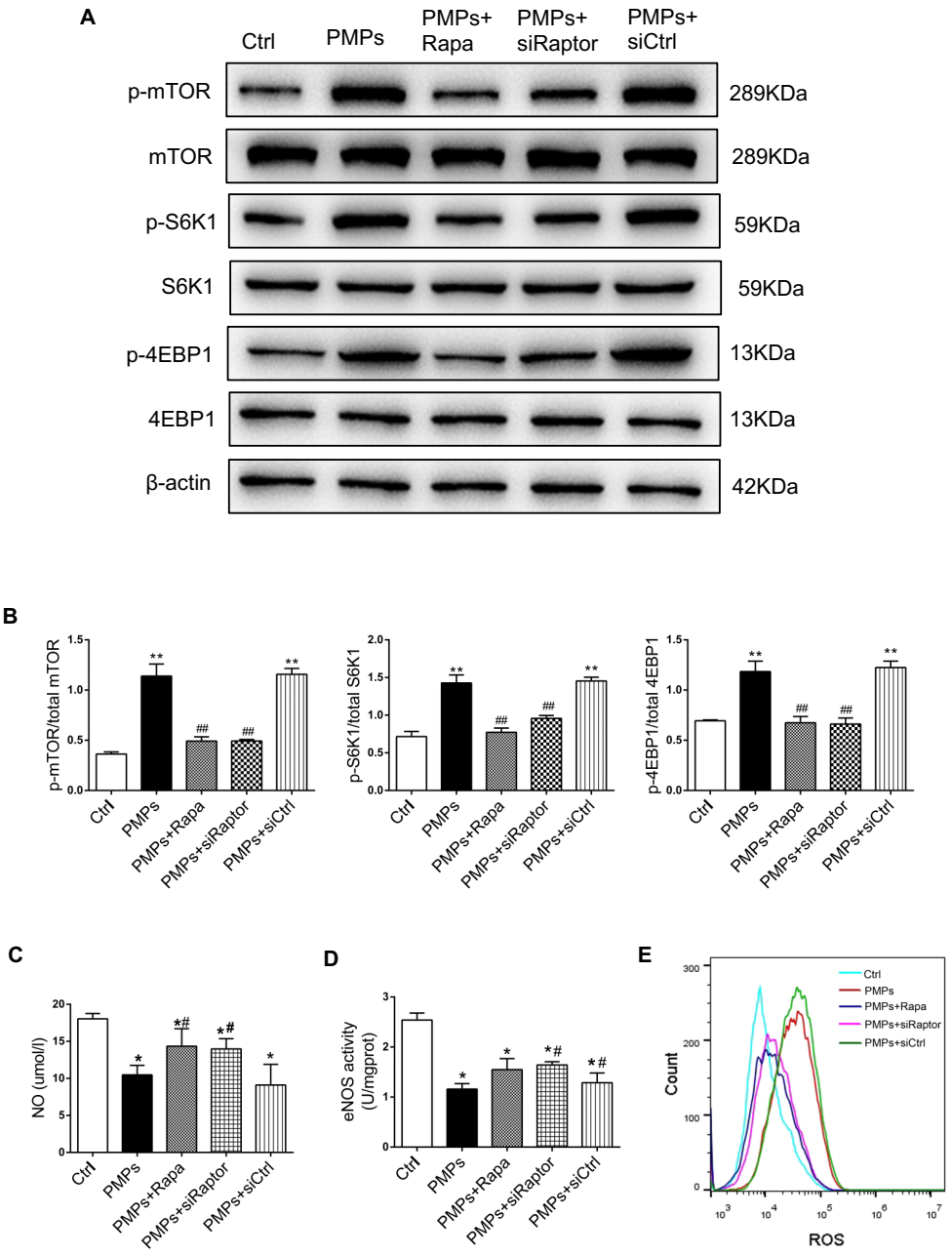
A
Ctrl
PMPs
PMPs+ Rapa
PMPs+ siRaptor
PMPs+ siCtrl
p-mTOR
289KDa
mTOR
289KDa
p-S6K1
59KDa
S6K1
59KDa
p-4EBP1
13KDa
4EBP1
13KDa
β-actin
42KDa
B
p-mTOR/total mTOR
p-S6K1/total S6K1
p-4EBP1/total 4EBP1
Ctrl
PMPs
PMPs+Rapa
PMPs+siRaptor
PMPs+siCtrl
C
NO (umol/l)
D
eNOS activity (U/mgprot)
E
Count
ROS
Ctrl
PMPs
PMPs+Rapa
PMPs+siRaptor
PMPs+siCtrl

F

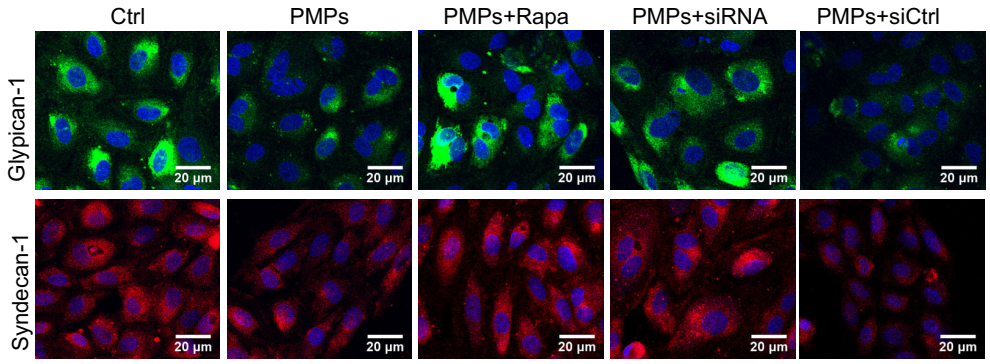
Ctrl
PMPs
PMPs+Rapa
PMPs+siRNA
PMPs+siCtrl
Glypican-1
Syndecan-1
20 μm

G

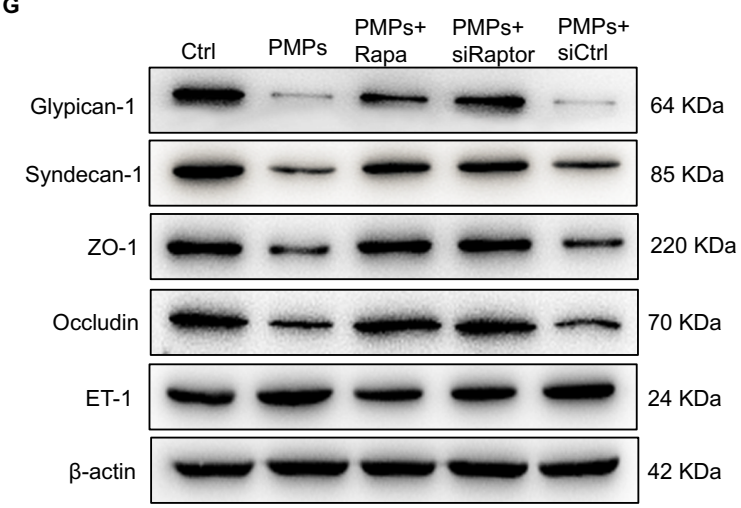
Ctrl
PMPs
PMPs+ Rapa
PMPs+ siRaptor
PMPs+ siCtrl
Glypican-1
64 KDa
Syndecan-1
85 KDa
ZO-1
220 KDa
Occludin
70 KDa
ET-1
24 KDa
β-actin
42 KDa

H

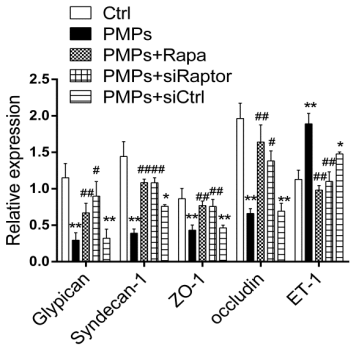
Ctrl
PMPs
PMPs+Rapa
PMPs+siRaptor
PMPs+siCtrl
Relative expression
Glypican
Syndecan-1
ZO-1
occludin
ET-1

I

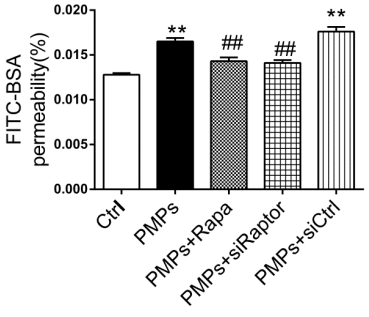
FITC-BSA permeability(%)
Ctrl
PMPs
PMPs+Rapa
PMPs+siRaptor
PMPs+siCtrl

Figure 6

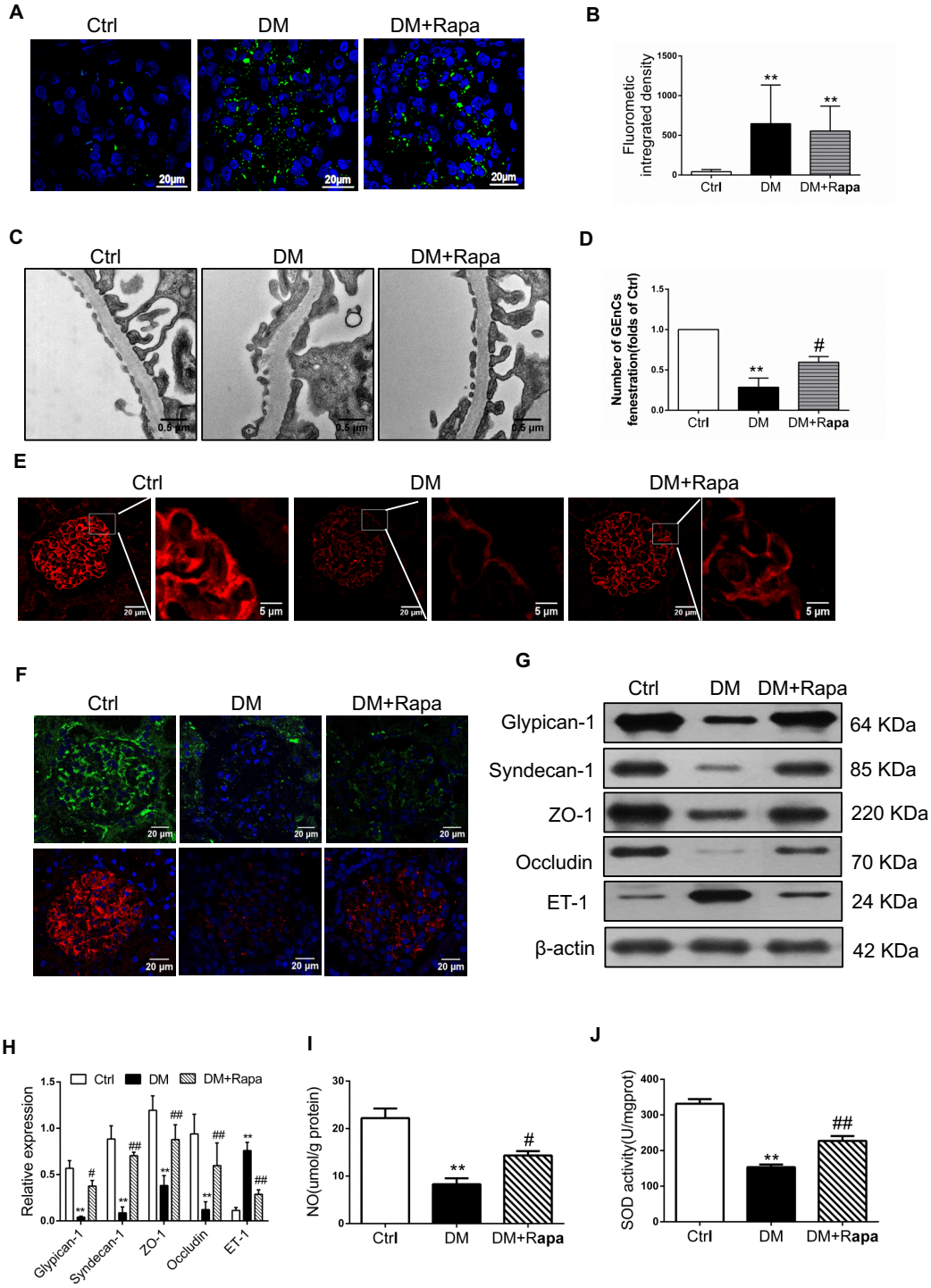
A
Ctrl
DM
DM+Rapa
20μm
B
Fluorometic intregrated density
1500
1000
500
0
**
**
Ctrl
DM
DM+Rapa
C
Ctrl
DM
DM+Rapa
0.5 μm
D
Number of GEnCs fenestration(folds of Ctrl)
1.5
1.0
0.5
0.0
**
#
Ctrl
DM
DM+Rapa
E
Ctrl
DM
DM+Rapa
20 μm
5 μm
F
Ctrl
DM
DM+Rapa
20 μm
G
Ctrl
DM
DM+Rapa
Glypican-1
64 KDa
Syndecan-1
85 KDa
ZO-1
220 KDa
Occludin
70 KDa
ET-1
24 KDa
β-actin
42 KDa
H
Ctrl
DM
DM+Rapa
Relative expression
1.5
1.0
0.5
0.0
Glypican-1
Syndecan-1
ZO-1
Occludin
ET-1
I
NO(umol/g protein)
30
20
10
0
**
#
Ctrl
DM
DM+Rapa
J
SOD activity(U/mgprot)
400
300
200
100
0
**
##
Ctrl
DM
DM+Rapa

Figure 7

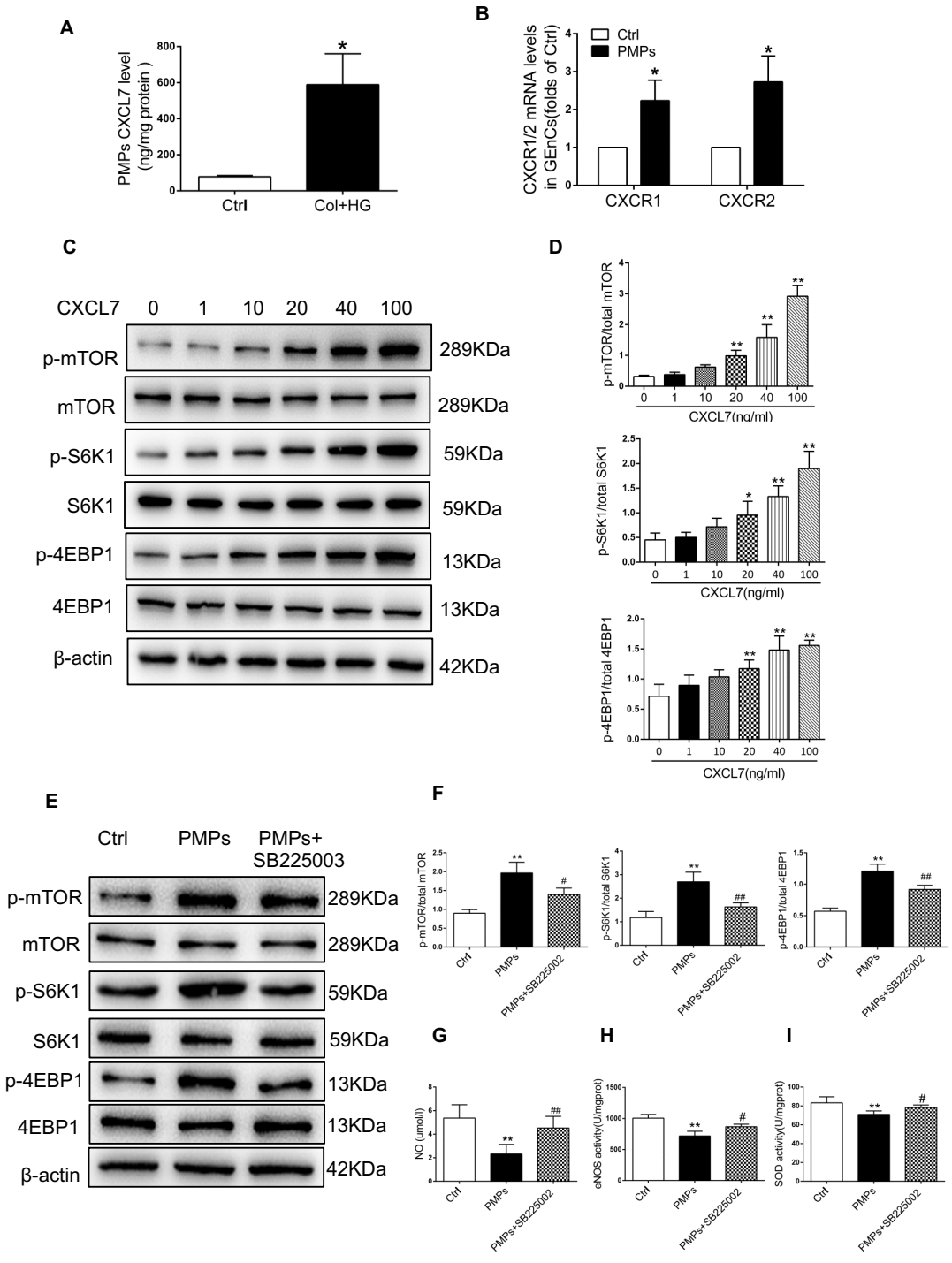
A
PMPs CXCL7 level (ng/mg protein)
800
600
400
200
0
Ctrl
Col+HG
B
CXCR1/2 mRNA levels in GEnCs(folds of Ctrl)
Ctrl
PMPs
CXCR1
CXCR2
C
CXCL7 0 1 10 20 40 100
p-mTOR
mTOR
p-S6K1
S6K1
p-4EBP1
4EBP1
β-actin
289KDa
289KDa
59KDa
59KDa
13KDa
13KDa
42KDa
D
p-mTOR/total mTOR
p-S6K1/total S6K1
p-4EBP1/total 4EBP1
CXCL7(ng/ml)
E
Ctrl
PMPs
PMPs+ SB225003
p-mTOR
mTOR
p-S6K1
S6K1
p-4EBP1
4EBP1
β-actin
289KDa
289KDa
59KDa
59KDa
13KDa
13KDa
42KDa
F
p-mTOR/total mTOR
p-S6K1/total S6K1
p-4EBP1/total 4EBP1
Ctrl
PMPs
PMPs+SB225002
G
NO (umol/l)
H
eNOS activity(U/mgprot)
I
SOD activity(U/mgprot)

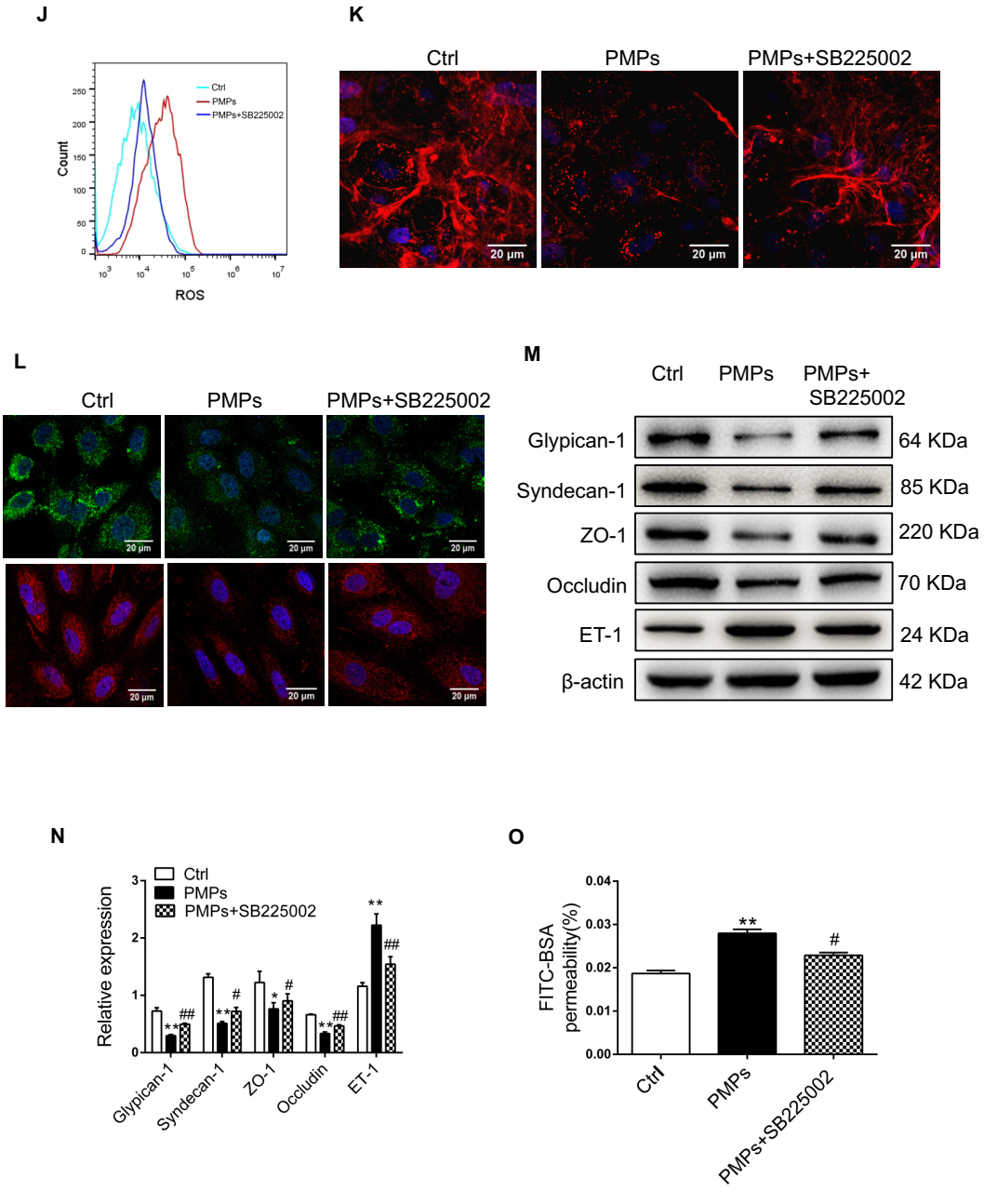
J
Ctrl
PMPs
PMPs+SB225002
Count
ROS
K
Ctrl
PMPs
PMPs+SB225002
20 μm
L
Ctrl
PMPs
PMPs+SB225002
20 μm
M
Ctrl
PMPs
PMPs+
SB225002
Glypican-1
Syndecan-1
ZO-1
Occludin
ET-1
β-actin
64 KDa
85 KDa
220 KDa
70 KDa
24 KDa
42 KDa
N
Ctrl
PMPs
PMPs+SB225002
Relative expression
Glypican-1
Syndecan-1
ZO-1
Occludin
ET-1
O
FITC-BSA permeability(%)
Ctrl
PMPs
PMPs+SB225002

Figure 8

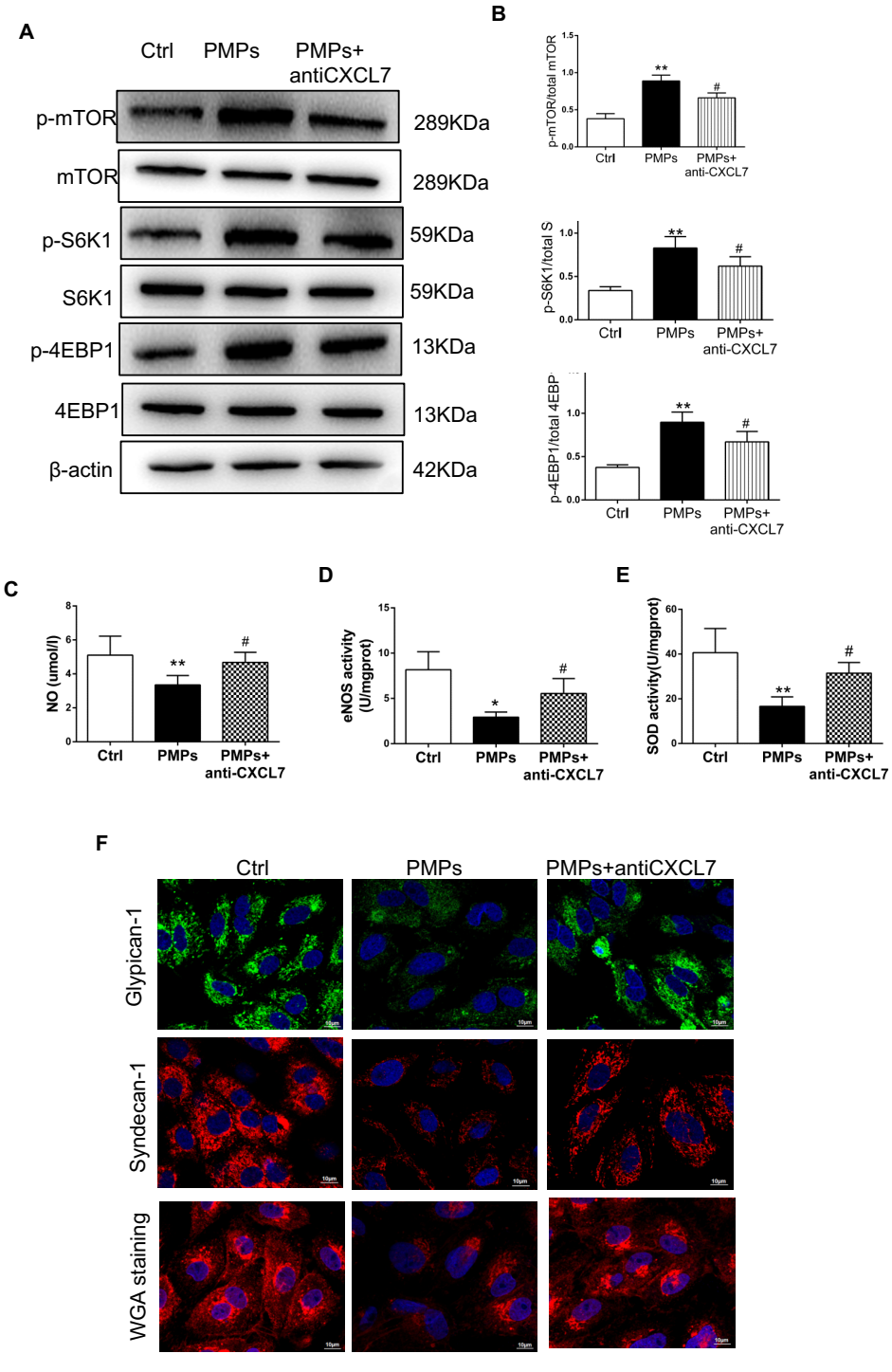
A
Ctrl
PMPs
PMPs+ antiCXCL7
p-mTOR
mTOR
p-S6K1
S6K1
p-4EBP1
4EBP1
β-actin
289KDa
289KDa
59KDa
59KDa
13KDa
13KDa
42KDa
B
p-mTOR/total mTOR
p-S6K1/total S
p-4EBP1/total 4EBP
Ctrl
PMPs
PMPs+ anti-CXCL7
C
NO (umol/l)
D
eNOS activity (U/mgprot)
E
SOD activity(U/mgprot)
F
Ctrl
PMPs
PMPs+antiCXCL7
Glypican-1
Syndecan-1
WGA staining

Figure 9

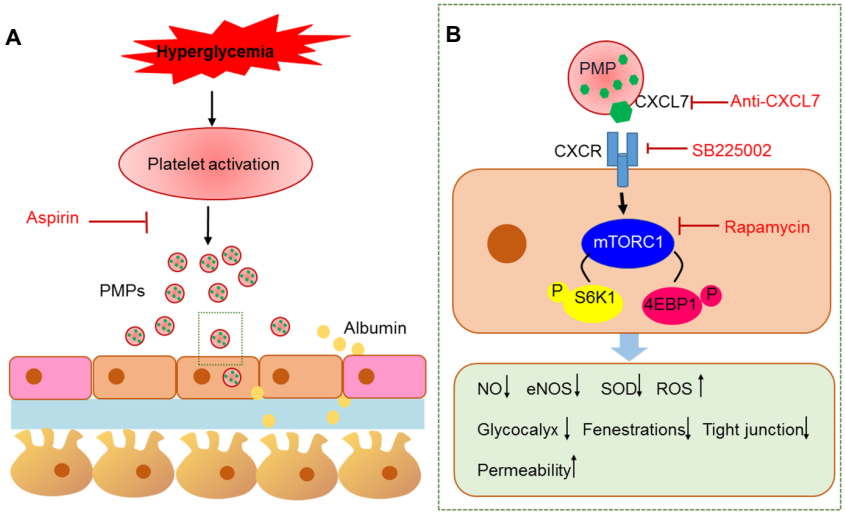
A
Hyperglycemia
Platelet activation
Aspirin
PMPs
Albumin
B
PMP
CXCL7
Anti-CXCL7
CXCR
SB225002
mTORC1
Rapamycin
P
S6K1
4EBP1
P
NO
eNOS
SOD
ROS
Glycocalyx
Fenestrations
Tight junction
Permeability